THE YOUNG PERSON'S GUIDE TO THE DATA

a survey lecture prepared for the
1968 AFOSR-IFP-Stanford Conference
on Computation of Turbulent Boundary Layers

Donald Coles
Professor of Aeronautics, California Institute of Technology
Consultant, The RAND Corporation*

I. INTRODUCTION

The business of this conference is to judge the present and potential value of various methods for calculating the development of the turbulent boundary layer in a pressure gradient. My task in this introductory lecture is to classify and criticize the available data, so that any comparison of measured and predicted quantities can include some estimate as to the quality and completeness of the various experiments. It goes without saying that I will try to do this without prejudicing any of the analytical ideas which may be considered by other speakers at this conference.

I have already dealt with the special case of flow at constant pressure, in an unpublished appendix to Rand Report R-403-PR (Coles 1962). My principal conclusions in that paper were:

(1) that a detailed classification can readily be carried out using the conventional similarity laws, although not much can be learned about the numerical value of the supposedly universal constants;

(2) that there apparently does exist a standard or normal configuration for the flow in question, at least when viewed in terms of the mean-velocity profile alone; and

(3) that among the factors which can adversely affect the quality of a standard boundary-layer flow, the most important are (a) three-dimensional effects and (b) poor judgment in the choice of tripping or thickening devices.

In the present survey, I will again sort through a large mass of data in an effort to detect patterns and conventions which aid in classification. It turns out that a weight has to be assigned to each experiment almost from the beginning, and that this weight is not necessarily the same when considering matters of technique as it is when choosing test cases for calculation or for publication in the proceedings of this symposium. From one point of view, those data turn out to be most useful in which only one factor is varied at a time. If the external conditions change, the instrumentation should remain the same, and conversely. From another point of view, there appears to be a certain level above which measurements can be described as being of professional quality. Such measurements are not only marked by good technique, but are usually also aimed at some particularly interesting or difficult area of the boundary-layer problem rather than at areas which have

* Any views expressed in this paper are those of the author. They should not be interpreted as reflecting the views of the RAND Corporation or the official opinion or policy of any of its governmental and private research sponsors.

been adequately explored in the past.

One obvious and venerable example is the contribution by Ludwieg and Tillmann (1949), who studied the effect of both positive and negative pressure gradients using the same impact-probe rake and heated-element instrumentation. Constructive work has also been done by Klebanoff and Diehl (1951) on the effect of initial conditions in flow at constant pressure, and by Bradshaw (1967) on the effect of initial conditions in a diffuser flow. I have several other favorite experiments; for instance, I will draw some delicate conclusions in section III, with the aid of some measurements by Schubauer and Klebanoff (1950) and by Bauer (1951), respectively, about possible effects of streamwise wall curvature and of probe size on apparent profile shape. In most cases these conclusions were not at issue in the original research, and the fact that they can be drawn at all is almost a definition of the professional experimental touch.

Circumstances have required certain measurements to be omitted, deliberately or otherwise. For almost all of the experiments discussed here, tabulated mean-velocity profiles and other data are available in the literature or have been supplied by the experimenters. In two cases, however, the data have been read from small figures in the original report, and their accuracy should be discounted accordingly. The first such case is the thesis by Gruschwitz (1931); the second is an NACA study of an airfoil boundary layer and wake by Mendelsohn (1947). Apparently it has been a practice at NACA to destroy raw data records after a lapse of a few years. Inasmuch as most of the NACA airfoil research of this period involved small models at relatively low Reynolds numbers, I doubt that the effort required to recover the data is worth while in general.

I should also mention several diffuser studies for which data have been provided by the authors, but which I have been forced to set aside, at least temporarily, because of lack of time. These data are potentially useful in support of the main body of material considered by this symposium. However, in my opinion they are not likely to lie near the center of attention, which I expect to be the problem of relaxation phenomena. In this class are the diffuser experiments by Sandborn and Slogar (1955), by Furuya (1958), by Sandborn (1959), by Rosenberg and Uram (1960), and by Spangenberg et al. (1967). I have also chosen for the present to omit data on reattaching flows obtained by Mueller (1961) and by Plate and Lin (1965), although measurements of this kind will undoubtedly play an important role in future research.

A number of measurements in axially-symmetric geometries are included in the test series but are not included in this survey. The reason is that I do not yet know how to handle an axially-symmetric coordinate system when the tests to be applied to the data are as systematic and delicate as the situation seems to allow -- and in fact to require -- in the case of plane flow.

Finally, I am compelled to comment on what I consider to be a general failure to exploit the advantages of hot-wire anemometers for measurement of mean as well as fluctuating quantities. As a consequence of this failure, all of the experiments considered in this survey include an unknown influence of the local turbu-

lence field on measurements of mean velocity by means of total-head tubes.* I suppose that data free of such effects will eventually become available in quantity, but this is not likely to happen soon. On the whole, therefore, I think that it is preferable at present to accept these effects as part of the data, rather than to attempt to remove them by unreliable or at any rate unproven methods.

II. SIMILARITY LAWS

In any survey of this kind, it is important to use the lightest analytical skeleton which will bear the weight of the data. For this and other reasons, I have again chosen to work with similarity laws, although I have little doubt that the same general conclusions could also be reached by other means.

My analysis begins with the idea that a typical boundary-layer flow can be viewed as a wake-like structure which is constrained by a wall. The wake-like behavior is apparent in the phenomena of intermittency and entrainment and in the sensitivity of the outer profile to pressure gradient. The wall constraint is felt mainly in the viscous sublayer and in the logarithmic part of the profile, and is closely related to the magnitude of the surface shearing stress.

The idea that there are two distinct scales in a turbulent boundary-layer flow is an old one, although quantitative expressions of this idea have evolved very slowly. A schematic representation of a typical profile is shown in the sketch. To the

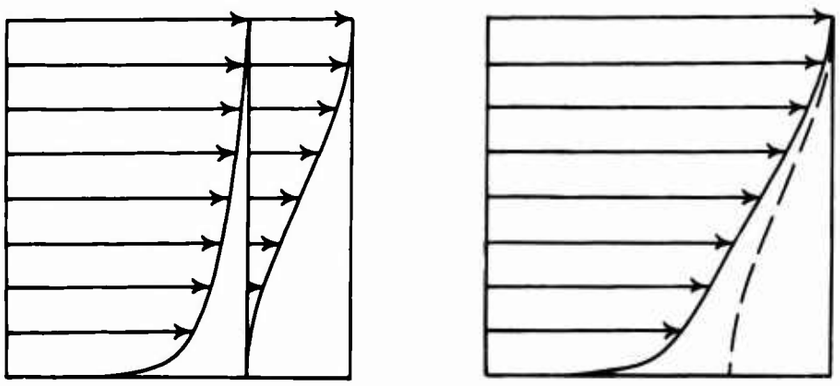

extent that the outer velocity boundary condition for the inner (wall) profile is the same as the inner velocity boundary condition for the outer (wake) profile, the turbulent boundary layer

* Newman (1951) made a partial correction for turbulence; both the corrected and uncorrected data have been obtained and are considered in this survey.

is a singular perturbation problem of classical type. In fact, we can claim to have discovered empirically the first two terms in a composite expansion, complete with logarithmic behavior. A corresponding physical view is that appreciable transfer of energy to the turbulent motion occurs at the largest scale, and that this energy is eventually converted to heat at the smallest scale (the sublayer thickness). Both of these notions become less opaque as the Reynolds number becomes very large, and it is possible to perceive dimly an analogy between the Kolmogorov inertial range and the logarithmic profile, both being manifestations of equilibrium at intermediate scales. It is also reasonable to think of the process of energy transfer as having a natural direction, and to expect a peculiar behavior when the initial energy distribution is highly abnormal.

The two similarity laws to be cited here are known as the law of the wall and the law of the wake. The most important property of the law of the wall is that it provides a quite plausible method for estimating surface friction.* The essence of this similarity law is perhaps best recognized from its use in describing the profile of the natural wind, for which neither an overall thickness nor an origin for the coordinate system can be defined. I am not aware of any convincing theoretical derivation of the law of the wall; i.e., one which does not at some stage fall back on dimensional analysis in order to adduce a viscous characteristic scale in a region of complete turbulence. Much of the empirical evidence in favor of the law comes from measurements in pipes, and in fact the commonly accepted value of Karman's constant is directly traceable to Nikuradse's pipe experiments. More recently, a thorough calibration of the device called a Preston tube has been carried out by Patel (1965) in pipe flow.** His results are shown as the lowest curve in figure 1. The coordinates are the usual ones for the law of the wall, with u the velocity corresponding to the observed dynamic pressure, and y the distance from the probe center to the wall (i.e., half the probe diameter). If the law of the wall is generally valid, these data should define the position of the first data point in any profile measured with a cylindrical probe.

The most important property of the law of the wake is that

* For historical purposes, it is worth noting that Ludwieg and Tillmann (1949) did not set out to show the general validity of the law of the wall, but stumbled on this result while investigating momentum-balance anomalies arising from use of the momentum-integral equation near separation. A careful reading of their description of the calibration of their heated element is also instructive, since this calibration was (to say the least) somewhat indirect.

** The major problems in such a calibration, given an undisturbed flow of high quality, are (a) to determine the static pressure which would exist in the absence of the probe, and (b) to minimize any non-local disturbances to the mean flow when the probe is present. These problems seem to have received careful attention in Patel's work.

it avoids a direct confrontation with the physical mechanism of shear turbulence. In order to use this law, it is not necessary to derive or even to explain the profile in a wake, but only to know what it looks like -- and also to believe that the same processes play a role in boundary-layer flow. In this sense, the concept was apparently first proposed by Hudimoto (1935). Hudimoto used a power law rather than a logarithmic law to isolate the part of the mean profile not directly affected by the wall, and he referred to the resulting function as jet-like rather than wake-like, but the spirit is essentially the same as the spirit of my own paper published 21 years later. Hudimoto wrote in English; so much for the hazards of publishing in an unreceptive atmosphere.

The similarity laws are explicitly displayed in my standard equation for the mean-velocity profile (Coles 1956),

$$\frac{\bar{U}}{u_\tau} = f\left(\frac{yu_\tau}{\nu}\right) + \frac{\Pi}{\kappa} w\left(\frac{y}{\delta}\right), \tag{1}$$

where $u_\tau^2 = \tau_w/\rho$. The function f (the law of the wall) has the form

$$f\left(\frac{yu_\tau}{\nu}\right) = \frac{1}{\kappa} \ln\left(\frac{yu_\tau}{\nu}\right) + C \tag{2}$$

outside the sublayer, which is to say for $yu_\tau/\nu > 50$. The constants κ and C are taken as 0.41 and 5.0 respectively, independent of pressure gradient. For analytical convenience I have represented the function w (the law of the wake) as

$$w\left(\frac{y}{\delta}\right) = 2 \sin^2\left(\frac{\pi}{2}\frac{y}{\delta}\right). \tag{3}$$

On putting $\bar{U} = \bar{U}_\infty$ and $y = \delta$ in the profile formula (1), the local friction law is obtained in the standard form

$$\frac{\bar{U}_\infty}{u_\tau} = \frac{1}{\kappa} \ln\left(\frac{\delta u_\tau}{\nu}\right) + C + \frac{2\Pi}{\kappa}. \tag{4}$$

Given κ, C, ν, and $\bar{U}_\infty$, the last equation evidently determines any one of the three parameters u_τ, δ, Π if the other two are known. Since equation (1) defines a two-parameter family of mean-velocity profiles, I have chosen to attack the data by finding values of two parameters δ and u_τ for each profile such that the rms deviation of the data from the formula (1) is minimized (data points for which $yu_\tau/\nu < 50$ or $y/\delta > 1$ are of course excluded). This procedure was originally developed in an attempt to salvage some data for which some or all of the mean-velocity profiles were incomplete (e.g., Riabouchinsky (1914), Perry (1966)). It was next applied, mostly out of a sense of pique, to several flow situations for which the profile formula (1) has been set aside by the authors or others as possibly inappropriate (e.g., Perry (1966), Stratford (1959)). Inasmuch as the procedure turned out to provide a very stable and well-controlled vehicle for classification, it was ultimately applied to the whole of the data.

It became apparent early in this process that the fitting region would have to be more carefully specified. One reason is that the formula (1) has an abrupt change in slope at the outer

edge of the layer, where $d(\bar{U}/u_\tau)/d(y/\delta)$ changes from $1/\kappa$ to 0. This is an obvious deficiency, and I will come back to it in section IV. At this stage of the development, it suffices to take the experimental existence of the corner into account by limiting the fitting region to the range $y/\delta < 0.9$ or less, partly to avoid unnecessary dispersion and partly to restrict the use of the formula to regions where it has some prospect of being accurate. The phrase "or less" means that the value 0.9 is satisfactory when the wake component is large, but has to be decreased to about 0.75 for flow at constant pressure, and to something like 0.6 as the wake component vanishes.

Moreover, I found in some but not all cases a significant disagreement between the data and formula (1) in the 10 to 15 percent of the profile nearest the wall, as illustrated for several flows in figure 1. On the assumption that this discrepancy could eventually be rationalized as experimental error, the lower limit of the fitting region was adjusted to exclude the data in question. I want to emphasize, however, that the upper and lower limits for fitting were not chosen capriciously for each profile, but were fixed for all the profiles of any one flow (except in the special case of flows undergoing relaxation, and occasionally also for data at very low Reynolds numbers).

The profile parameters obtained from this process include C_f, Π, and δ, all determined in a self-consistent way. Note that C_f is now being determined by a fit of the central part of the complete profile to the full formula (1), rather than by a fit of the inner profile alone to the law of the wall (cf the remarks in the "Memorandum on Data Selection" which follows this survey paper). The main effect of the change is usually to reduce C_f by perhaps one or two percent. Note also that the parameters Π and δ are now differently and more realistically defined than was the case in my 1956 paper, since the existence of a discontinuity in slope at $y = \delta$ is now being taken into account.

To sum up: points near the edge of the boundary layer have been omitted from the fitting operation on the ground that the data are correct but the formula is wrong, and points near the wall have been omitted on the tentative ground that the formula is correct but the data are wrong, due (say) to effects of wall interference and/or effects of local strong turbulence. For the majority of the flows studied, this procedure seems to be entirely adequate. The fit is usually good enough so that the results are quite insensitive to minor changes in the size of the fitting region. In fact, a typical rms scatter of the data about the fitted curve in the fitted region is two or three parts in 1000 (referred to free-stream velocity). This conclusion may come as a pleasant surprise to some experimenters; it also provides a challenge for theoreticians who work independently of the profile formula (1). After careful study, I have not found any consistent pattern in the remaining small discrepancies, and so I cannot suggest a better analytical representation for either of the functions f or w than the simple functions used here.

THE VARIOUS PROFILE PARAMETERS AS DETERMINED BY THE METHODS JUST DESCRIBED ARE LISTED IN TABLE I AT THE END OF THIS PAPER.

Finally, I have reexamined the problem of evaluating integral thicknesses for profiles which are defined by relatively few data points near the wall, especially when the Reynolds number is also small. The problem is illustrated in figure 2, which shows the ratio $H_{32} = \delta_3/\theta$ (energy/momentum) plotted against the ratio $H_{12} = \delta^*/\theta$ (displacement/momentum). The upper curve, labelled (a), shows values taken directly from the standard tables supplied to the predictors, together with some additional data points obtained by the same methods. I did not expect that the data would define a single curve, because there must be a Reynolds-number dependence in such a presentation; but in fact the scatter turns out to be wholly unacceptable. Matters are improved in the middle curve (b), which is the same as (a) except that I have deleted all data for profiles which lack experimental definition for $\bar{U}/\bar{U}_\infty$ less than 1/2. As might be expected, the offending data points correspond to some or all of the profiles in flows 1400, 1800, 3100, 6100, and 6200, among others. These data cover a wide range of Reynolds numbers, and the difficulty must therefore arise in our original choice of an unrealistic interpolation method for the numerical integration near the wall. In any event, it is clear that very little use can be made of these particular data until some better interpolation scheme is specified.

For the sake of consistency, therefore, the integral thicknesses have been recalculated for all of the flows listed in Table I after replacing the experimental data near the wall by standard functions, with the results shown in curve (c) of figure 2. The standard sublayer profile is a slight revision of one which I have used before, and takes into account recent measurements by Liu (1966), Bakewell (1966), and others. All that needs to be known about the standard sublayer profile in order to reproduce the tabulated thicknesses is that

$$\int_0^{50} (\bar{U}/u_\tau)\, d(yu_\tau/\nu) = 540.6;$$

$$\int_0^{50} (\bar{U}/u_\tau)^2\, d(yu_\tau/\nu) = 6546;$$

$$\int_0^{50} (\bar{U}/u_\tau)^3\, d(yu_\tau/\nu) = 82770.$$

The gap between $yu_\tau/\nu = 50$ and the first point used in fitting is filled in by formula (1) with the $(\sin)^2$ function replaced by one term in y^2, and the integration is then continued numerically by the usual parabolic interpolation scheme. I consider the revised values of displacement, momentum, and energy thickness to be substantially more credible than the original ones, inasmuch as interpolation between measured points near the wall is now on a sounder basis.

THE INTEGRAL THICKNESSES AND RELATED QUANTITIES DETERMINED BY THE METHODS JUST DESCRIBED ARE ALSO LISTED IN TABLE I AT THE END OF THIS PAPER.

III. FLOWS IN OR NEAR EQUILIBRIUM

In this section I will consider only flows for which the profile formula of section II definitely provides a good representation of the data. This class seems to include nearly all equilibrium or near-equilibrium flows and nearly all flows of airfoil or diffuser type. I have not always limited myself to data which are being officially considered at this conference, and in some cases I have changed the emphasis slightly.

Figures 3 and 4 show the result of the fitting operation for several flows which are close to equilibrium in the sense of Clauser's definition. What is plotted is the wake component alone. That is, the fitting operation described in section II has first been carried out for the central 50 to 80 percent of the profile, and the logarithmic part has then been subtracted out.

In almost all cases, there are difficulties in the region close to the wall, even though points for which yu_τ/ν is less than 50 are omitted. These difficulties may well be an instrumentation problem; they will be discussed in more detail at the end of this section, when more data have been put in evidence. The seeming increase in scatter in figure 4 as the pressure gradient becomes more negative is due to the fact that a smaller fraction of the velocity profile -- in the worst case, as little as five percent -- is being displayed in the figures. That the notion of a wake component still makes sense under these conditions is a compliment both to the skill of the experimenters and to the quality of the similarity laws.

There are also systematic discrepancies, especially in figure 4, near the outer edge of the layer; this is the corner effect mentioned in section II. In order to look at this effect more closely, I have converted the data of figure 4 into residuals, or differences between the data and the profile formula, with the result shown in figure 5. The ordinate is $\Delta\bar{U}$ made dimensionless with u_τ, on the assumption that the corner effect is associated most closely with the law of the wall. The maximum error in velocity is about one percent of $\bar{U}_\infty$, and the area represented by the corner in figure 5 is typically $\int(\Delta\bar{U}/u_\tau)d(y/\delta) \sim 0.1$, compared to an area of $(1 + \Pi)/\kappa$ for the displacement thickness in the same units. It follows that ignoring the corner effect may lead to errors in displacement and momentum thickness of at most about 4 and 5 percent, respectively. There is a definite suggestion in figure 5 that the corner effect becomes more pronounced as Π approaches zero, perhaps because of deeper penetration of the region of intermittency into the layer as dp/dx becomes large and negative. Unfortunately, speculation on this point is almost useless as long as the free-stream turbulence level (presumably low for all of the data in figure 5) and its effects on the profile are unknown. An immediate conclusion is that it is highly desirable to know the free-stream turbulence level in such experiments, and almost essential to know the intermittency distribution.

On the premise that it is sensible to look for something where it is large rather than where it is small, I have also evaluated the wake function for a number of diffuser-like flows as

shown in figure 6. These flows are all developing toward separation and are therefore characterized by a strong flux of energy in the natural direction; i.e., from the mean flow to the turbulence. In all cases, the fit to the wake law can be modestly described as superb over perhaps 90 to 95 percent of the layer. In particular, Stratford's two flows (1959) are in no way distinguished from the others, and the wall-wake concept is reinforced rather than refuted by these particular data.*

I have also found a number of anomalies, explainable or otherwise, in some of the measurements included in this survey. One of the most intriguing is a small but definite change in the shape of the profiles in the Schubauer-Klebanoff experiment (1950) at the station where the surface curvature begins. This change is documented in figure 7, where I have plotted the wake component and the residuals, the latter in units of $\Delta\bar{U}/\bar{U}_\infty$, for two regions of the flow. The difference in profile shape is almost certainly not due to neglect of the "barely detectable" static pressure difference through the layer, since this difference is unlikely to be larger than $\rho\bar{U}_\infty^2\delta/R$, and ought to be much smaller. With δ/R in the range from .007 to .017, it would be very generous to expect as much as one percent error in mean velocity when the pressure is assumed constant. Moreover, this error would presumably be monotonic through the layer and correspondingly difficult to detect. On the contrary, I believe that the effect shown in figure 7 is almost certainly due to a stabilizing action of the centripetal force on the turbulence. Another property of the Schubauer-Klebanoff experiment raises a different question. Especially in the downstream region, there is rather more scatter in the profile data from one station to another than in any one profile by itself. The measurements extended over a considerable time, and the reference velocity was adjusted from day to day to maintain a constant unit Reynolds number, regardless of changes in atmospheric temperature and pressure. Although the same technique has been used by other experimenters before and since, I think that for a turbulent flow, which is almost by definition highly insensitive to Reynolds number, it would be better to reproduce some non-viscous parameter such as a local or overall pressure coefficient.

Some other anomalies are illustrated in figures 8 and 9. In each figure, the top curve shows all of Gruschwitz's profiles for which Π is greater than unity (1931; Messreihe 4 and 5), and the matter of interest is the abnormally large corner effect at the edge of the layer. Whether this effect is due to the low Reynolds number, to a presumably high free-stream turbulence level, or to the small probe size, is not clear. The next two curves refer to two of Bell's flows (1966) for which there seems to be a definite disagreement with the standard wake function. I think the source of the discrepancy is clear in this case, since the surface was heated, and the density was therefore assumed too large in deducing

* Both Stratford and Clauser had to cope with unusual difficulties in measurement because of the low velocities in their flows; note that the dynamic pressure in the free stream in the downstream part of Clauser's second flow was only about 2 mm of alcohol, whereas Bauer, working with water, could dispose of nearly 200 mm of mercury.

velocity from dynamic pressure near the wal' (this explanation could of course be tested directly, by using the measured temperature profiles, but I have not done so). It should be noted that Bell's probe was very wide compared to its height; in fact, almost two-dimensional, but Perry's measurements (1966) with the same instrumentation* show no distortion of the profile shape (cf figure 6c). Another case of distortion occurs in Tillmann's ledge flow (1945). Curve (d) in figure 9 shows the residual error for the last few stations in this flow, the profiles being so nearly logarithmic that the wake component is too small to be displayed in figure 8. Because there is no such distortion in the nearly equivalent measurements by Klebanoff and Diehl (1951) behind a ¼-inch rod, I prefer to classify Tillmann's results as anomalous data rather than as solid evidence of a breakdown of the wall-wake formula.

Finally, a comment about the three flows studied by Bauer (1951). These are nominally the same flow. However, the probe used to obtain the data for 40° slope was four times larger than the probe used for 20° and 60° slope. There is a slight complication in that the behavior of the parameter Π in the upstream region for 60° slope, documented in Table I of this paper, suggests that a tripping device may have been present. The real point, however, is that the values of Π for the flow with 40° slope lie generally below those for the other two flows in the downstream region ($\Pi \sim 0.26$ compared to 0.30), and the corner function is slightly weaker in figure 5. I suspect, therefore, that the effects of differences in probe size and/or probe damping may sometimes be detectable in the intermittent region.

It remains to face the question of experimental discrepancies near a wall. My own conclusions, after careful study, are mostly negative. Firstly, I do not approve of an uncritical application of the Young-Maas correction for displacement effect; and secondly, I do not know how to estimate errors in impact-probe measurements of mean velocity when the local turbulence level is high. There is no question that both kinds of error are real. For instance, one primitive but unusual experiment has been reported in which the sign of both errors should be reversed; this is the moving-belt flow of Riabouchinsky (1914). His data are shown as the lowest curve in figures 8 and 9 and as the top curve in figure 1. Although the data are far from definitive, they suggest that the discrepancy does in fact change sign.

On the other hand, why is figure 6 (diffuser flows) generally clean near the wall, while figures 3 and 4 (equilibrium flows) are not? It is likely (Perry 1966, Bell 1966) that a wide rectangular probe is less subject to error near a wall than a round probe, and may even indicate too low a velocity. The rationale is that an effectively two-dimensional probe produces local separation, thus

---

* One wry comment here; Bell and Perry used an elegant automatic plotting system, which produced profiles directly in logarithmic coordinates. However, several numerical errors in their transcription of these plots suggest that automation, once begun, ought to be carried to completion rather than subjected to fallible human intervention.

impairing the pressure recovery, while a round probe produces a flow deflection toward the wall (due to induction by a trailing vortex system), thus sensing a pressure which is too high. However, Bradshaw (1966) takes another position on the question of the effect of probe shape, and the evidence from his own measurements is ambiguous (cf figures 3b, 3c, 3e, 6e).

I have one other observation on probe technique. The evidence in figures 1, 4, 5, and 6 suggests that a rake or multiple probe, as used at Göttingen (Ludwieg and Tillmann 1949, Wieghardt 1944), is not more subject to error than a single probe. If so, such a rake has obvious advantages of speed, accuracy, and convenience. Note, however, that the evidence of Tillmann's data (1945) in figure 9 does not support this conclusion.

Clarification of these problems in instrumentation may eventually come from a more professional attitude toward use of linearized hot-wire anemometers, or from developments in statistical marker or tracer methods (including laser doppler techniques). Pending clarification, I think that it is probably a waste of time to attempt detailed mean-velocity measurements near a wall using conventional impact-probe instrumentation.

This is not to say that measurements in thin boundary layers, where there is no room to encounter this difficulty, recommend themselves except perhaps for special problems such as transition. Although it is demonstrably easier to achieve a nearly two-dimensional mean flow in thin layers, I doubt that much information would be lost by suppressing all data obtained in turbulent low-speed boundary layers less than 1 cm thick. It is clearly important in turbulence research to work at high Reynolds numbers; the data considered here suggest that a 5-foot model in a stream at 50 feet per second is marginal, while a 15-foot model in a stream at 100 feet per second is not. I am also struck by the scarcity of measurements in water, despite the access which is thereby provided to large Reynolds numbers and to powerful methods of flow visualization.

IV. A LOCAL FRICTION LAW

A formula proposed by Ludwieg and Tillmann (1949) is commonly used as a local friction law to connect the three variables C_f, R_δ, and $H = \delta^*/\theta$. In practice, the chief virtue of this formula (which I view as essentially an empirical power-law relationship of a fairly sophisticated kind) is that it is explicitly soluble for each of its three variables. This survey paper seems an appropriate place to test the usefulness of equation (4) above as an alternative and more rational formula for the estimation of local friction coefficient, and I want to digress briefly for this purpose.

The boundary-layer thickness δ can be eliminated from equation (4) by first defining integral displacement and momentum (and sometimes energy) thicknesses in the usual way,

$$\frac{\delta^* \bar{U}_\infty}{\delta u_\tau} = \int_0^\infty \left(\frac{\bar{U}_\infty - \bar{U}}{u_\tau}\right) d\frac{y}{\delta} \qquad (5)$$

$$\frac{(\delta^* - \theta)\bar{U}_\infty^2}{\tau_w/\rho} = \int_0^\infty \left(\frac{\bar{U}_\infty - \bar{U}}{u_\tau}\right)^2 d\,\frac{y}{\delta} \qquad (6)$$

and so on. The particular profile functions (2) and (3) then imply

$$\kappa\,\frac{\delta^*\bar{U}_\infty}{\nu/u_\tau} = 1 + \Pi \qquad (7)$$

$$\kappa^2\,\frac{(\delta^* - \theta)\bar{U}_\infty^2}{\tau_w/\rho} = 2 + 2\left[1 + \frac{1}{\pi}\,\mathrm{Si}(\pi)\right]\Pi + \frac{3}{2}\,\Pi^2 \qquad (8)$$

etc. In principle, elimination of u_τ/ν and Π from the parametric system (4), (7), (8) yields a relationship between $C_f = 2u_\tau^2/\bar{U}_\infty^2$, $R_\theta = \bar{U}_\infty\theta/\nu$, and $H = \delta^*/\theta$. In practice, complete elimination of Π is prevented by the transcendental form of the original equation (4). After considering a variety of possible parametric representations, I prefer one in which the variables remain bounded, namely

$$\left(\frac{H}{H-1}\right)\frac{1}{\kappa f} = F(\Pi) \qquad (9)$$

$$\left(\frac{H}{H-1}\right)\left(1 - \frac{1}{\kappa f}\,\ell n|R_{\delta^*}|\right) = K(\Pi) \qquad (10)$$

$$F(\Pi) = \frac{1 + \Pi}{2 + 2\left[1 + \frac{1}{\pi}\,\mathrm{Si}(\pi)\right]\Pi + \frac{3}{2}\,\Pi^2} \qquad (11)$$

$$K(\Pi) = (\ell n\,\kappa + \kappa c + 2\Pi - \ell n|1 + \Pi|)F(\Pi) \qquad (12)$$

where $f = \bar{U}_\infty/u_\tau$ and $\mathrm{Si}(x) = \int_0^x \frac{\sin u}{u}\,du = -x\int_0^1 \ell n\, y \cos xy\, dy$.

The complete function F(K) defined by equations (11) and (12) is the closed curve* shown in the small insert at the top of figure 10. In the first quadrant, the parameter Π increases from -1 at the origin, where $\delta^* = 0$, to $+\infty$ at the point (F, K) = (0, 4/3), where $u_\tau = 0$. This is the region of interest for the purposes of this boundary-layer survey, and it is enlarged to form the main part of figure 10.

Values of f, H, and R_{δ^*} for about 450 profiles are available from Table I. (Both an inner fit and an outer fit may be listed for certain profiles; it is the outer fit which I am considering here). These values have been used to compute F and K from the defining equations (9) and (10), with the results shown in

* I have used the sign convention that f is positive if $\bar{U}_\infty$ and τ_w have the same sense, and is negative otherwise. With this convention, the absolute value signs in equations (10) and (12) allow the formulas to be extended to wall jets and to separated flow, although it is doubtful that the particular functions f and w defined by equations (2) and (3) will always be the appropriate ones in such cases. I have not considered the problem of representing laminar flows or free shear flows in the figure.

figure 10a. The large scatter at low values of Π is obviously caused by my use of a logarithmic profile in the sublayer in evaluating the expressions (7) and (8). For example, if the sublayer profile is corrected by an amount $\Delta\bar{U}/u_\tau$ which depends on yu_τ/ν, an extra term of the form "constant/($\delta^* u_\tau/\nu$)" will appear on the right in equation (7). For my favorite sublayer profile, the constant is about 65 κ, or about 27, and the correction is unimportant if either Π or $\delta^* u_\tau/\nu$ is large. When the correction term is moved to the left side of the equation (for the sake of the single-parameter formulation), the final result is

$$\kappa \frac{(R_{\delta^*} - 65)}{\delta^* u_\tau/\nu} = 1 + \Pi \qquad (7a)$$

The corresponding correction to equation (8) is messier, but it turns out that reducing R_{δ^*} by 65 is again a good approximation to the required correction in the whole range of the data, and is essentially exact when $f \sim 17$. I have therefore recomputed F and K from equations (9) and (10) after reducing R_{δ^*} by $65\nu/\bar{U}_\infty$ in both H and R_{δ^*}. The result is shown in figure 10b. The scatter is now much less, and the remaining discrepancies seem to be caused mostly by neglect of the corner effect in evaluating the integrals (see section III and figures 5 and 9). If $\Delta\bar{U}/u_\tau$ in the corner region is a function of y/δ, then the right-hand side of equation (7) or (7a) for δ^* should be further modified by adding a constant of order 0.1 to the sum $1 + \Pi$. The correction is again unimportant if Π is large. A similar small change will occur in the coefficients on the right in equation (8) for H. However, I have not worked out any details from this point onwards, because I suspect that the observed corner effect depends strongly on the intermittency distribution and perhaps weakly on the probe damping characteristics. The intermittency distribution, in turn, must be affected both by free-stream turbulence level and by the energy history of the flow. Among the noisiest measurements in figure 10b, incidentally, are those by Schubauer and Klebanoff (1950), presumably because of profile distortion due to surface curvature.

I should comment on the obviously circular nature of this treatment of the local friction law. The same profile formula (1) has been used both to determine $f = \bar{U}_\infty/u_\tau$ (say) and also to test the results for consistency by way of figure 10. However, there are two extenuating circumstances. The first is that the question of momentum balance has not come up explicitly in preparing figure 10, so that if necessary the quantity u_τ can be interpreted simply as a well defined and useful parameter for the mean velocity profile, much like the parameter Π. For example, the product Πu_τ (i.e., the strength of the wake component) might be a quite reliable indicator of the local rate of production of large-scale turbulent energy. Whether or not u_τ is equal to $\sqrt{\tau_w/\rho}$ is irrelevant from this point of view, and in fact no decision on this point can be made for most of the flows considered here. The second extenuating circumstance is that I am looking for patterns in the available data. In order to succeed, I have had to reject much of the experimental evidence for the mean-velocity profile in and near the sublayer. I do not think that this procedure will eventually be proved to be wrong; but if it is, the errors involved are neither large nor beyond repair.

As a final illustration of the use of a local friction law to test the quality of the available experimental data, I have computed C_f as a function of R_θ for several flows which are nominally in equilibrium (Π = constant). The sublayer correction is included in the computation, but the corner correction is not, and a possible tendency for the wake component to weaken at low Reynolds number is also ignored (see Coles 1962, Appendix A, for a discussion of this tendency in the case of flow at constant pressure). The results are shown in figure 11a. When the momentum balance for the various flows is taken into account, it appears that the case of flow at constant pressure (Wieghardt 1944) is under good control, as is one case of equilibrium flow in a negative pressure gradient (Bauer 1951). However, the four equilibrium flows in positive pressure gradients (Clauser 1954, Bradshaw 1966) may all be somewhat shaky, especially as regards the numerical value of any pressure-gradient parameter which is used to characterize the fact of equilibrium.

V. ABNORMAL AND RELAXING FLOWS

I now have to say a little about flows for which the methods of section II break down. In principle, there is more to be learned from a minority of cases where a general procedure fails than from a majority of cases where it does not. Unfortunately, the quality and completeness of the data tend to deteriorate in this area, and the conclusions thus tend to be less conclusive.

For ten of the 45 flows listed in Table I*, I have carried out an inner fit as well as an outer fit for some or all of the profiles. By "inner fit" I mean that a few points near the wall but outside the sublayer have been put on the logarithmic line, in the same manner originally used to prepare the data for this conference, and with much the same results. My hope was that different characteristic scales (u_τ and δ, say) could be attached to the inner and outer portions of the profile, and that their relative rates of change might reveal something about the dynamical processes occurring in the flow. However, I have little confidence in the parameters derived from the inner fit, in view of what I believe are serious experimental difficulties in measurement of mean-velocity profiles near a wall in regions of high turbulence level. In fact, I am convinced of a real failure of the similarity laws only for three cases (2400, 5200, 5300).

The data suggest that there are at least two different circumstances which can lead to failure of the wall-wake concept, even when the boundary-layer approximation itself is not called into question. One abnormal situation is the presence of very large pressure forces of either sign. The natural result seems to be a rotational flow, in which the turbulent stresses are negligible and the mean motion is determined by pressure forces alone, so that the total pressure is constant on mean streamlines. Such behavior is well known from experience with three-dimensional mean

* Six of these ten flows (1500, 2400, 5600, 5800, 5900, 6000) are relaxing from a relatively high turbulence energy level toward a lower one, at essentially constant pressure (cf figure 11b). The other four flows are responding to a strong local pressure gradient, which may be either positive (5200, 5300) or negative (1700, 1800).

flow and from studies of relaminarization in strong negative pressure gradients, where, however, the situation may be further complicated by suicidal tendencies in the turbulence structure. Weak instances of a trend toward relaminarization are provided by the second flow ($\beta = -0.53$) of Herring and Norbury (1967) and by portions of Gruschwitz's two flows (1931), although the similarity laws seem to be still valid for these examples. A stronger instance, involving a response to a very large positive pressure gradient, occurs in the early part of Stratford's two flows (1959), in which at least the second and third profiles show a hopeless lack of similarity in the inner region. The latter two flows thus provide a particular challenge for the predictors at this conference.

The second abnormal situation occurs in the relaxation process which follows an abrupt change in the external or boundary conditions, a process which is known to involve large and slowly decaying distortions in the mean flow. This topic is to be covered by Professor Tani in another paper, but a few remarks may not be out of place here.

Despite the fact that instrumentation errors near a wall tend to be larger and less systematic in relaxing flows, it is clear that the rate of accommodation of the inner and outer regions of the flow is not the same. The large-scale motion associated with the law of the wake reacts slowly, while the small-scale motion associated with the law of the wall adjusts itself continuously to local conditions. During this process, the similarity laws may still provide a good approximation for the mean-velocity profile. Note also that there is sometimes a tendency for a flow which is relaxing toward equilibrium to overshoot the mark and then to recover. This tendency is illustrated in figure 11b, the left portion of which shows the behavior of the local friction coefficient in several flows at constant pressure. The overshoot is most marked when there is complete separation and reattachment, as in the ledge flow studied by Tillmann (1945) and in the flow with ¼-inch rod studied by Klebanoff and Diehl (1951). The profiles in the second of these two examples seem to lie within the scope of the general profile representation, while the profiles in the first perhaps do not, as already pointed out in figure 9. The reason is unknown. I regret that the intermittency properties of flows of this type have not been measured, especially in the region where the mean-velocity profile is closely logarithmic. The contrast with the situation near relaminarization should be striking. Note also that the friction history is incomplete for the sequence of three flows with rough-smooth transition studied by Klebanoff and Diehl (1951). Inasmuch as the value of C_f is initially large in the region of roughness, each flow has already overshot the final equilibrium state once before the data even begin. As the Reynolds number increases in this sequence of three flows, the final recovery process becomes relatively slower, presumably because of an increasing separation between the energy-containing scales and the dissipative scales at the higher Reynolds numbers.

Figure 11b also shows a sequence of three flows studied by Bradshaw (1967). In each case, the pressure gradient changes rapidly from zero to a standard positive near-equilibrium value near the first station, and the three flows differ mainly in the

initial Reynolds number. I view the last four profiles in flow A (6400) with great suspicion (since they seem to correspond to an altered initial condition), but I have no real grounds for rejecting these data out of hand.

Figure 11b also shows the evolution of the relaxing flow $a = -0.255 \rightarrow 0$ of Bradshaw and Ferriss (1965). The mean-velocity data are precise enough to establish that the similarity laws definitely fail for this flow, but I am not convinced that the measured profiles are free of error in and near the sublayer. The most that I have been willing to do with the data is to compare, in figure 12, the results of an outer fit for the relaxing flow and for the corresponding equilibrium flow. At three stations where profiles were measured in both flows, I have cross-hatched the area representing the difference. Although the boundary-layer thicknesses and Reynolds numbers are not strictly compatible, I believe that this difference in profile shape is probably a useful measure of local distortion. Note that in this experiment, as in most of the others shown in figure 11b, the relaxation process is far from complete at the last experimental station.

Finally, I have included one other example of a relaxing flow among the data of this survey paper. This is a study by Mendelsohn (1947) of a boundary layer developing into a wake. The experiment is unsatisfactory in that (a) the Reynolds number is quite small; (b) the measurements are a little ragged, and do not extend far enough into the wake; and (c) there may be some difficulty with the boundary-layer approximation near the trailing edge. Nevertheless, these measurements seem to be the best available at the moment.

The quantity of interest is the center-line velocity defect in the wake, or in the equivalent wake in the case of boundary-layer flow. This equivalent wake is the dashed line in the right-hand profile sketch in section II of this paper. The data points in a boundary layer, of course, do not lie on this line, but on the composite profile. According to equation (4), the strength of the wake component (referred to the local free-stream velocity) is $2\Pi u_\tau / \kappa U_\infty$. This quantity was determined by fitting the outer part of each boundary-layer profile to the wall-wake formula, and this fitting process was continued downstream into the wake without regard for the changed nature of the actual flow. The results are shown in figure 13 by the circles (open in the boundary-layer region; filled in the wake region). To repeat; it is the intersection of the dashed curve in the sketch with the line $y = 0$ which is denoted by the circles in figure 13, and this intersection is a purely hypothetical one which stands or falls with the whole wall-wake concept of the profile. In the fully developed wake, on the other hand, the data points do lie on the dashed line. Hence the outer part of each wake profile was fitted to the wake function alone, and this fitting process was also continued upstream into the boundary layer. The results are shown in figure 13 by the triangles (open if the flow is actually a wake, filled if it is not). Finally, the actual measured velocity defect on the centerline of the wake is denoted by open squares.

Figure 13 shows that the effect of removing the wall constraint is felt quickly throughout the layer. The adjustment of

the initial wake flow near the plane of symmetry is relatively rapid when compared either to pressure-driven changes in the original boundary layer or to mixing-dominated decay in the final wake. This rapid adjustment includes small and intermediate scales, but not large scales; the final wake seems to evolve smoothly from the hypothetical wake profile associated with the boundary-layer flow, rather than from the boundary-layer profile itself. If this conclusion is correct, it follows that the expected rapid decrease in displacement thickness near the trailing edge can be readily estimated from the condition that the momentum thickness remains constant. I believe that flow situations of this kind should certainly be examined more closely and carefully, and that such a re-examination might well include the case of unsymmetrical flow also considered by Mendelsohn.

VI CONCLUSION

I have already commented at length on various regularities and irregularities which seem to characterize the behavior of turbulent boundary layers, given substantial differences in the experimental regime, the instrumentation, and the observer. I assume that anyone preparing a prediction scheme for this conference will be conscious of variations in the quality of the data, and will want to adjust his analytical machinery so as to reproduce certain flow situations more accurately than others. I have therefore recorded in the adjacent table my present opinion as to the relative value for this purpose of the available measurements. Where there is a choice among several nearly equivalent experiments, I recommend that data listed toward the left in the table be given more weight than data listed toward the right. Where there is no such choice, and where the need for information is sufficiently urgent, I have no doubt that new measurements will eventually become available.

1300	5700	1600^{a}	4500^{d}	1100^{b}	4700^{d}
1400^{a}	5800	1700^{a}	4800^{ad}	1200^{b}	5200^{c}
2400^{d}	5900	1800^{be}		1500^{cd}	
2600^{e}	6000	2100_{a} (x<20 ft)^{d}		2100_{c} (x>20 ft)^{bd}	
3000^{e}	6100	2300^{a}		2200^{cd}	
3100^{e}	6200	2500^{a}	4900^{ad}	2800^{cd}	5300^{c}
3200	6300	2700^{a}	5400^{a}	2900^{b}	5500^{ad}
3300		3500^{b}	5600^{a}	4200^{bd}	6400^{d}
		4400^{a}	6500^{d}	4600^{d}	

(a) Small discrepancies in momentum balance for part or all of flow.
(b) Large discrepancies in momentum balance in region of rising pressure, probably due in part to omission of turbulence terms.
(c) Large discrepancies in momentum balance for part or all of flow, probably due mostly to three-dimensionality.
(d) Considerable station-to-station scatter in profile parameters.
(e) Abnormally low Reynolds number; sublayer profile may be crucial.

THE DISCUSSION OF THIS PAPER IS INCLUDED IN THE MONDAY MORNING DISCUSSION IN VOLUME I

REFERENCES

Bakewell, H. Jr. 1966 An experimental investigation of the viscous sublayer in turbulent pipe flow. Dept. Aerosp. Eng., Penn. State Univ., Contr. Rep. Nonr (G)-00043-65.

Bauer, W. J. 1951 The development of the turbulent boundary layer on steep slopes. Ph.D. Thesis, State Univ. Iowa.

Bell, J. 1966 Forced turbulent convective heat transfer from a flat plate in adverse pressure gradients. M. Eng. Sci. Thesis, Univ. Melbourne.

Bradshaw, P. and Ferriss, D. H. 1965 The response of a retarded equilibrium turbulent boundary layer to the sudden removal of pressure gradient. NPL Aero Rep. 1145.

Bradshaw, P. 1966 The turbulence structure of equilibrium boundary layers. NPL Aero Rep. 1184.

Bradshaw, P. 1967 The response of a constant-pressure turbulent boundary layer to the sudden application of an adverse pressure gradient. NPL Aero Rep. 1219.

Clauser, F. H. 1954 Turbulent boundary layers in adverse pressure gradients. J. Aero. Sci. 21, 91-108.

Coles, D. 1956 The law of the wake in the turbulent boundary layer. J. Fluid Mech. 1, 191-226.

Coles, D. 1962 The turbulent boundary layer in a compressible fluid. RAND Corp., Rep. R-403-PR.

Furuya, Y. 1958 Experiments and theory on flow in the diffuser. Mem. Fac. Eng., Nagoya Univ., 10, 1-41.

Gruschwitz, E. 1931 Die turbulente Reibungsschicht in ebener Strömung bei Druckabfall und Druckanstieg. Ing.-Arch. 2, 321-346.

Herring, H. J. and Norbury, J. F. 1967 Some experiments on equilibrium turbulent boundary layers in favorable pressure gradients. J. Fluid Mech. 27, 541-549.

Hudimoto, Busuke 1935 On the turbulent boundary layer with pressure rise and fall. Mem. Coll. Eng., Kyoto Imperial Univ.,9, 1-17.

Klebanoff, P. S. and Diehl, Z. W. 1951 Some features of artificially thickened fully developed turbulent boundary layers with zero pressure gradient. NACA TN 2475.

Liu, C., Kline, S., and Johnston, J. 1966 An experimental study of turbulent boundary layer on rough walls. Dept. Mech. Eng., Stanford Univ., Rep. MD-15.

Ludwieg, H. and Tillmann, W. 1949 Untersuchungen über die Wandschubspannung in turbulenten Reibungsschichten. Ing.-Arch. 17, 288-299.

Mendelsohn, R. 1947 Wind-tunnel investigation of the boundary layer and wake and their relation to airfoil characteristics - NACA 65$_1$-012 airfoil with a true contour flap and a beveled-trailing-edge flap. NACA TN 1304.

Mueller, T. J. 1961 On separation, reattachment, and redevelopment of turbulent boundary layers. Ph.D. Thesis, Univ. Ill.

Newman, B. G. 1951 Some contributions to the study of the turbulent boundary layer near separation. Australia, Dept. Supply, Rep. ACA-53.

Patel, V. C. 1965 Calibration of the Preston tube and limitations on its use in pressure gradients. J. Fluid Mech. 23, 185-208.

Perry, A. E. 1966 Turbulent boundary layers in decreasing adverse pressure gradients. J. Fluid. Mech. 26, 481-506.

Plate, E. and Lin, C. 1965 The velocity field downstream from a two-dimensional model hill. Parts I, II. Coll. Eng., Colo. State Univ., Contr. Rep. DA-AMC-36-039-63-G7.

Riabouchinsky, D. 1914 Étude expérimentale sur le frottement de l'air. Boul. de L'Institute Aerodynamique de Koutchino, 5, 51-72.

Rosenberg, M. and Uram, E. 1960 Data on incompressible turbulent boundary layers in adverse pressure gradients. United Aircr. Corp. Res. Labs., Rep. M-0949-3.

Sandborn, V. A. and Slogar, R. J. 1955 Longitudinal turbulent spectrum survey of boundary layers in adverse pressure gradients. NACA TN 3453.

Sandborn, V. A. 1959 Measurements of intermittency of turbulent motion in a boundary layer. J. Fluid Mech. 6, 221-240.

Schubauer, G. B. and Klebanoff, P. S. 1950 Investigation of separation of the turbulent boundary layer. NACA TN 2133.

Schubauer, G. B. and Spangenberg, W. B. 1958 Forced mixing in boundary layers. J. Fluid Mech. 8, 10-32.

Spangenberg, W. G., Rowland, W. R., and Mease, N. E. 1967 Measurements in a turbulent boundary layer maintained in a nearly separating condition. General Motors Symp., Fluid Mechanics of Internal Flow, Elsevier, 110-151.

Stratford, B. S. 1959 An experimental flow with zero skin friction throughout its region of pressure rise. J. Fluid Mech. 5, 17-35.

Tillmann, W. 1945 Untersuchungen über Besonderheiten bei turbulenten Reibungsschichten an Platten. Z. W. B., K. W. I., U & M 6627.

Wieghardt, K. and Tillmann, W. 1944 Zur turbulenten Reibungsschicht bei Druckansteig. Z. W. B., K. W. I., U & M 6617.

TABLE 1

PROFILE PARAMETERS FROM FIT TO WALL-WAKE FORMULA; INTEGRAL THICKNESSES

(1) 'ymin' and 'ymax' always denote first and last data points used in fitting operation
(2) 'inner fit' denotes fit to wall law alone (i.e., Clauser fit)
(3) 'resid' is rms deviation of fitted data from formula (1) after velocity is normalized to unity in free stream
(4) Integrals are always computed using standard sublayer formula between wall and y = ymin
(5) delta.utau/nu can be evaluated either from delta, U, Cf, and nu, or from U/utau and PI using formula (4)

x	U	Cf	ymin	ymax	delta	U/utau	PI	resid	displ	mom	energy	Rmom
LUDWIEG and TILLMANN - mild positive pressure gradient												1100
nu = 0.155 cm2/sec; fitted between y/delta = 0.10, 0.90												
m	m/sec		cm	cm	cm				cm	cm	cm	
.782	33.90	.002795	.4	2.0	2.5249	26.75	.643	.0009	.3818	.2798	.4950	6120
1.282	32.60	.002466	.4	3.0	3.6241	28.48	.867	.0019	.5762	.4158	.7296	8746
1.782	30.70	.002201	.6	4.0	4.9519	30.14	1.111	.0017	.8494	.6082	1.0640	12046
2.282	28.60	.001983	1.0	5.0	6.3373	31.76	1.380	.0015	1.1650	.8139	1.4083	15017
2.782	27.10	.001794	1.0	7.0	8.0672	33.39	1.646	.0010	1.5671	1.0749	1.8465	18793
3.132	26.05	.001651	1.0	8.0	9.3425	34.80	1.902	.0021	1.9016	1.2775	2.1774	21470
3.332	25.75	.001583	1.5	9.0	10.3182	35.55	2.022	.0022	2.1471	1.4342	2.4401	23827
3.532	24.85	.001493	1.5	10.0	11.4146	36.60	2.219	.0017	2.4553	1.6160	2.7349	25908
3.732	24.50	.001402	1.5	11.0	12.2901	37.77	2.445	.0017	2.7405	1.7744	2.9861	28047
3.932	24.05	.001315	1.5	12.0	13.6553	38.99	2.668	.0023	3.1425	2.0060	3.3601	31125
4.132	23.60	.001223	2.0	13.0	15.0669	40.44	2.943	.0024	3.5849	2.2453	3.7359	34187
4.332	23.10	.001148	2.0	15.0	16.7497	41.73	3.182	.0025	4.0949	2.5272	4.1851	37663
LUDWIEG and TILLMANN - strong positive pressure gradient												1200
nu = 0.150 cm2/sec; fitted between y/delta = 0.10, 0.90 except as noted by * *												
m	m/sec		cm	cm	cm				cm	cm	cm	
.782	33.00	.002893	.4	2.0	2.2404	26.29	.597	.0015	.3373	.2479	.4395	5454
1.282	31.20	.002465	.4	2.5	3.2835	28.49	.924	.0015	.5456	.3916	.6863	8145
1.782	28.80	.002038	.5	4.0	4.6112	31.33	1.423	.0039	.8778	.6055	1.0445	11626
2.282	27.10	.001878	1.0	5.0	6.0842	32.63	1.603	.0011	1.1910	.8133	1.3962	14694
2.782	24.65	.001529	1.0	7.0	8.3722	36.16	2.266	.0020	1.8547	1.2039	2.0295	19785
3.132	23.45	.001299	1.5	9.0	10.1331	39.23	2.866	.0026	2.4459	1.5240	2.5356	23826
3.332	22.90	.001179	1.5	10.0	11.8662	41.19	3.224	.0024	2.9752	1.8119	2.9912	27661
3.532	22.43	.000976	1.5	12.0	13.6581	45.27	4.048	.0021	3.7292	2.1587	3.5111	32279
3.732	22.10	.000827	2.0	13.0	15.5399	49.17	4.831	.0019	4.5068	2.4962	4.0104	36777
3.932	22.13	.000491	*3.0*	17.0	19.8932	63.81	7.838	.0022	6.7304	3.2607	5.0730	48107
LUDWIEG and TILLMANN - negative pressure gradient												1300
nu = 0.154 cm2/sec; fitted between y/delta = 0.15, 0.60 except as noted by * *												
m	m/sec		cm	cm	cm				cm	cm	cm	
.782	11.52	.004448	*.3*	.7	1.2235	21.21	.288	.0046	.1983	.1383	.2652	1034
1.282	13.38	.004412	.3	.9	1.5427	21.29	.117	.0046	.2100	.1524	.2732	1324
1.782	15.61	.004111	.3	.9	1.5750	22.06	.205	.0025	.2226	.1621	.2300	1643
2.282	17.85	.003986	.3	1.0	1.8771	22.40	.128	.0030	.2379	.1770	.3181	2051
2.782	20.20	.003707	.4	1.0	1.8203	23.23	.269	.0019	.2578	.1916	.3437	2513
3.132	22.07	.003628	.4	1.2	2.0028	23.48	.234	.0008	.2656	.1986	.3564	2846
3.332	22.90	.003624	.4	1.2	2.0416	23.49	.209	.0014	.2647	.1990	.3578	2959
3.532	23.70	.003584	.4	1.2	2.0733	23.69	.229	.0024	.2732	.2059	.3705	3169
3.732	25.13	.003569	.4	1.2	2.0763	23.67	.194	.0016	.2647	.2005	.3613	3272
3.932	25.80	.003405	.4	1.2	2.1344	24.24	.295	.0023	.2932	.2213	.3978	3707
4.132	26.40	.003392	.4	1.2	2.3391	24.28	.248	.0010	.3025	.2284	.4129	3933
4.332	27.50	.003348	.4	1.2	2.2760	24.44	.278	.0010	.3038	.2307	.4154	4120
WIEGHARDT - 33.0 m/sec												1400
nu = 0.151 cm2/sec; fitted between y/delta = 0.125, 0.750 except as noted by * *												
m	m/sec		cm	cm	cm				cm	cm	cm	
.087	33.00	.005288	.05	*.2*	.2381	19.45	.167	.0045	.0385	.0253	.0445	554
.187	33.00	.004138	.1	.3	.4716	21.99	.407	.0022	.0780	.0536	.0942	1171
.287	33.00	.003744	*.2*	.4	.6632	23.11	.492	.0003	.1084	.0756	.1330	1653
.387	33.00	.003478	.2	.6	.8360	23.98	.573	.0009	.1377	.0965	.1695	2109
.487	33.00	.003381	.2	.7	.9923	24.32	.564	.0012	.1602	.1137	.2002	2484
.637	33.00	.003289	.2	.8	1.1994	24.66	.546	.0019	.1885	.1352	.2387	2955
.787	33.00	.003114	.2	1.0	1.4100	25.34	.619	.0020	.2245	.1610	.2838	3519
.937	33.00	.003091	.4	1.2	1.6176	25.44	.571	.0014	.2489	.1810	.3204	3956

TABLE 1 (CONT'D)

x	U	Cf	ymin	ymax	delta	U/utau	PI	resid	displ	mom	energy	Rmom
1.087	33.00	.003000	.4	1.2	1.8151	25.82	.600	.0008	.2805	.2044	.3617	4467
1.237	33.00	.002919	.4	1.5	2.0139	26.20	.634	.0026	.3109	.2264	.4001	4947
1.437	33.00	.002850	.4	1.5	2.2755	26.49	.637	.0017	.3483	.2550	.4511	5572
1.687	33.00	.002800	.4	1.8	2.6352	26.73	.616	.0023	.3919	.2887	.5117	6309
1.987	33.00	.002730	.4	2.0	3.0166	27.07	.625	.0014	.4470	.3311	.5877	7236
2.287	33.00	.002663	.5	2.5	3.5039	27.40	.625	.0021	.5075	.3767	.6687	8233
2.587	33.00	.002630	.5	2.5	3.8153	27.58	.621	.0012	.5520	.4119	.7323	9001
2.887	33.00	.002591	1.0	3.0	4.2096	27.78	.618	.0006	.6038	.4526	.8057	9890
3.187	33.00	.002568	1.0	3.0	4.5990	27.91	.602	.0007	.6498	.4891	.8718	10689
3.487	33.00	.002519	1.0	3.0	4.9241	28.18	.627	.0022	.7009	.5279	.9410	11536
3.787	33.00	.002488	1.0	3.0	5.2102	28.35	.638	.0023	.7452	.5620	1.0022	12282
4.087	33.00	.002469	1.0	4.0	5.6040	28.46	.626	.0027	.7905	.5971	1.0676	13071
4.387	33.00	.002431	1.0	4.0	6.0617	28.68	.636	.0013	.8528	.6455	1.1519	14106
4.687	33.00	.002435	1.0	4.0	6.4332	28.66	.601	.0010	.8863	.6745	1.2062	14741
4.987	33.00	.002422	1.0	5.0	6.9244	28.74	.581	.0010	.9343	.7129	1.2757	15580

TILLMANN - ledge 1500
nu = 0.152 cm2/sec; fitted between y/delta = 0.15, 0.75 upstream of ledge; fitted between y/delta = 0.25, 0.75 downstream of ledge
INNER FIT DENOTED BY ( )

m	m/sec		cm	cm	cm				cm	cm	cm	
.487	17.70	.003704	.2	.8	1.2976	23.24	.500	.0068	.2135	.1489	.2615	1734
.787	17.70	.003329	.4	1.2	1.7402	24.51	.641	.0055	.2938	.2065	.3628	2405
1.087	17.70	.003267	.4	1.5	2.2127	24.74	.573	.0040	.3492	.2493	.4392	2903
1.436	17.70	.003158	.6	2.0	2.7288	25.16	.563	.0053	.4182	.3012	.5315	3508
1.737	17.70	.002867	.5	2.0	3.1813	26.41	.766	.0049	.5338	.3820	.6717	4449
2.186	18.68	.000362	1.5	3.0	4.7318	74.29	10.872	.0069	1.8759	.7790	1.1927	9574
2.211	18.50	.000547	1.5	3.0	4.8740	60.47	7.926	.0018	1.7825	.8123	1.2590	9887
2.236	18.29	.000771	1.5	3.0	4.9041	50.94	5.890	.0049	1.6481	.8205	1.2926	9873
2.286	18.09	.001220	1.5	3.0	5.2821	40.48	3.600	.0018	1.4704	.8334	1.3516	9918
2.386	17.79	.001733	1.5	4.0	5.9352	33.97	2.127	.0020	1.3367	.8538	1.4346	9993
2.586	17.70	.002333	2.0	5.0	7.1028	29.28	1.003	.0047	1.1956	.8568	1.4983	9975
2.886	17.70	.002653	2.5	6.0	8.6390	27.45	.500	.0014	1.1606	.8825	1.5796	10276
3.186	17.70	.002762	3.0	7.0	10.3840	26.91	.286	.0031	1.2148	.9481	1.7144	11040
3.486	17.70	.002877	3.0	8.0	11.6973	26.36	.105	.0017	1.1801	.9375	1.7078	10917
3.786	17.70	.002854	4.0	8.0	12.4894	26.47	.096	.0020	1.2558	1.0022	1.8285	11670
4.086	17.70	.002896	4.0	10.0	13.0230	26.28	.032	.0031	1.2554	1.0113	1.8531	11777
4.386	17.70	.002786	4.0	11.0	14.0861	26.79	.108	.0078	1.4206	1.1359	2.0732	13227
4.686	17.70	.002779	4.0	10.0	15.0575	26.83	.082	.0029	1.4560	1.1662	2.1298	13580
4.986	17.70	.002743	4.0	11.0	15.4421	27.00	.109	.0028	1.5491	1.2434	2.2728	14480
5.286	17.70	.002751	4.0	11.0	15.9284	26.96	.084	.0035	1.5661	1.2609	2.3077	14683
2.186	18.68	.000291	(.5)	(.5)	*******	82.90	******	.0000	1.9271	.7545	1.1531	9272
2.211	18.50	.000569	(.5)	(.5)	*******	59.26	******	.0000	1.7938	.8095	1.2528	9852
2.236	18.29	.000839	(.5)	(.5)	*******	48.81	******	.0000	1.6492	.8216	1.2936	9886
2.286	18.09	.001407	(.5)	(.5)	*******	37.71	******	.0000	1.4463	.8372	1.3628	9964
2.386	17.79	.001977	(.5)	(1.0)	*******	31.80	******	.0066	1.3037	.8526	1.4406	9979
2.586	17.70	.002570	(.5)	(1.0)	*******	27.90	******	.0002	1.1556	.8457	1.4888	9848
2.886	17.70	.002901	(.5)	(1.0)	*******	26.26	******	.0037	1.1118	.8836	1.5563	10054
3.186	17.70	.002977	(.5)	(1.0)	*******	25.92	******	.0006	1.1658	.9264	1.6856	10787
3.486	17.70	.003028	(.5)	(1.0)	*******	25.70	******	.0021	1.1423	.9192	1.6821	10704
3.786	17.70	.003071	(.5)	(1.0)	*******	25.52	******	.0001	1.1884	.9669	1.7768	11259
4.086	17.70	.003005	(.5)	(1.0)	*******	25.80	******	.0008	1.2187	.9911	1.8225	11541
4.386	17.70	.002878	(1.0)	(1.5)	*******	26.36	******	.0028	1.3791	1.1133	2.0395	12984
4.686	17.70	.002878	(1.0)	(1.5)	*******	26.36	******	.0018	1.4134	1.1437	2.0968	13318
4.986	17.70	.002838	(1.0)	(1.5)	*******	26.55	******	.0016	1.5027	1.2186	2.2362	14191
5.286	17.70	.002818	(1.0)	(1.5)	*******	26.64	******	.0016	1.5322	1.2426	2.2805	14470

RIAROUCHINSKY (profiles viewed from moving wall) 1600
nu = 0.1455 cm2/sec; fitted between y/delta = 0.10, 0.55 except as noted by * *

m	m/sec		cm	cm	cm				cm	cm	cm	
2.00	16.00	.002335	*2.36*	7.02	12.817	29.27	.735	.0024	1.8602	1.3933	2.4751	15321
4.00	16.00	.002021	2.79	12.94	23.591	31.46	.915	.0043	3.5118	2.6294	4.6574	28914
6.00	16.00	.001944	3.63	18.02	34.308	32.07	.864	.0069	4.8511	3.6842	6.5671	40513
8.00	16.00	.001912	4.06	21.40	39.875	32.34	.848	.0046	5.5626	4.2443	7.5755	46672
10.00	16.00	.001915	4.48	23.94	43.911	32.33	.797	.0059	5.9551	4.5736	8.1786	50296
10.94	16.00	.001894	4.90	24.78	45.283	32.50	.819	.0043	6.1867	4.7512	8.4905	52247

GRUSCHWITZ - Messreihe 4 1700
nu = 0.152 cm2/sec; fitted between y/delta = 0.20, 0.80 except as noted
OUTER FIT DENOTED BY | |; INNER FIT DENOTED BY ( )

cm	m/sec		cm	cm	cm				cm	cm	cm	
49.30	32.82	.004191	.120	.300	.4114	21.85	.449	.0014	.0708	.0479	.0840	1035
51.70	31.56	.003818	.142	.380	.5250	22.89	.586	.0015	.0932	.0652	.1104	1312

TABLE 1 (CONT'D)

x	U	Cf	ymin	ymax	delta	U/utau	Pi	resid	displ	mom	energy	Rmom
54.30	30.16	.003449	.182	.450	.6262	24.08	.789	.0024	.1193	.0800	.1389	1588
56.70	29.05	.003225	.192	.500	.7297	24.90	.916	.0025	.1421	.0944	.1629	1803
59.30	28.19	.003014	.232	.662	.8526	25.76	1.046	.0026	.1706	.1127	.1939	2090
61.70	27.49	.002889	.222	.700	.9571	26.31	1.124	.0029	.1948	.1284	.2205	2322
64.30	26.83	.002760	.250	.800	1.0717	26.92	1.216	.0004	.2209	.1447	.2476	2554
66.70	26.27	.002726	.262	.900	1.1415	27.08	1.232	.0033	.2343	.1535	.2626	2654
71.70	26.20	.002795	.400	1.000	1.2532	26.75	1.112	.0016	.2476	.1654	.2847	2851
76.70	26.86	.003141	.370	.900	1.3360	25.23	.727	.0042	.2262	.1576	.2750	2784
79.30	27.42	.003311	.340	.900	1.2883	24.58	.587	.0039	.2057	.1453	.2550	2620
81.70	28.42	.003477	.380	.900	1.2884	23.98	.436	.0024	.1921	.1387	.2457	2593
84.30	29.64	.003677	.280	1.000	1.2948	23.32	.262	.0032	.1768	.1308	.2340	2551
86.70	30.78	.003803	|.400|	.950	1.2543	22.93	.171	.0031	.1613	.1204	.2164	2439
89.30	32.08	.003894	|.500|	.950	1.1966	22.66	.113	.0010	.1461	.1093	.1966	2307
91.70	33.45	.004025	|.400|	.750	1.2058	22.29	.004	.0023	.1355	.1028	.1862	2263
94.30	34.78	.004167	|.400|	.850	1.2189	21.91	-.108	.0018	.1234	.0946	.1720	2164
96.70	35.85	.004254	|.350|	.950	1.1513	21.68	-.146	.0023	.1146	.0883	.1611	2083
86.70	30.78	.003972	(.160)	(.400)	******	22.44	*****	.0088	.1555	.1178	.2127	2385
89.30	32.08	.004222	(.100)	(.240)	******	21.77	*****	.0124	.1364	.1046	.1899	2207
91.70	33.45	.004349	(.080)	(.180)	******	21.44	*****	.0088	.1271	.0987	.1803	2173
94.30	34.78	.004437	(.080)	(.180)	******	21.23	*****	.0072	.1166	.0911	.1668	2084
96.70	35.85	.004469	(.070)	(.170)	******	21.16	*****	.0060	.1091	.0854	.1566	2013

GRUSCHWITZ - Messreihe 5 1800
nu = 0.148 cm2/sec; fitted between y/delta = 0.20, 0.80 except as noted by • •
OUTER FIT DENOTED BY | |; INNER FIT DENOTED BY ( )

cm	m/sec		cm	cm	cm				cm	cm	cm	
49.30	25.64	.004517	.110	.280	.4188	21.04	.367	.0026	.0711	.0476	.0834	824
51.70	25.75	.004702	.110	.310	.4705	20.62	.211	.0037	.0718	.0493	.0870	857
54.30	26.93	.004599	.130	.380	.5898	20.85	.128	.0025	.0817	.0577	.1028	1051
56.70	27.64	.004899	|.200|	.380	.5333	20.21	.017	.0008	.0693	.0492	.0880	919
59.30	29.79	.005012	|.200|	.380	.5061	19.98	-.047	.0007	.0620	.0443	.0794	892
61.70	32.46	.005206	|.190|	.370	.4680	19.60	-.137	.0026	.0547	.0397	.0718	871
64.30	36.77	.005506	|.180|	•.360•	.4209	19.06	-.272	.0014	.0423	.0308	.0558	764
66.70	41.47	.005635	|.140|	.270	.3724	18.84	-.321	.0024	.0358	.0261	.0474	731
69.35	48.33	.005925	|.090|	.170	.2769	18.37	-.358	.0040	.0270	.0197	.0359	644
71.70	54.57	.005818	|.090|	.150	.2239	18.54	-.274	.0004	.0247	.0179	.0326	661
74.35	60.29	.005625	|.100|	.180	.2341	18.86	-.272	.0013	.0254	.0187	.0342	764
76.70	62.13	.004884	|.080|	.180	.2265	20.24	.047	.0051	.0321	.0232	.0418	973
79.35	60.76	.004076	.060	.170	.2523	22.15	.442	.0011	.0443	.0310	.0548	1271
81.70	57.62	.003488	.070	.220	.3196	23.94	.757	.0026	.0612	.0415	.0724	1616
84.35	53.63	.002826	.090	.280	.4251	26.60	1.248	.0042	.0919	.0598	.1024	2167
86.70	50.10	.002384	.170	.360	.5432	28.96	1.686	.0011	.1265	.0790	.1332	2676
89.35	47.04	.001921	.250	.550	.7098	32.26	2.314	.0021	.1793	.1064	.1759	3381
91.70	44.81	.001553	.300	.600	.8559	35.89	3.040	.0007	.2378	.1342	.2186	4062
94.35	42.92	.001314	.400	.800	1.0423	39.01	3.646	.0011	.3046	.1657	.2670	4806
96.70	41.67	.001173	.400	.900	1.1955	41.29	4.087	.0035	.3626	.1930	.3094	5434
56.70	27.64	.004945	(.080)	(.200)	******	20.11	*****	.0043	.0687	.0490	.0877	914
59.30	29.79	.005125	(.080)	(.200)	******	19.76	*****	.0141	.0601	.0432	.0778	870
61.70	32.46	.005270	(.070)	(.190)	******	19.48	*****	.0151	.0530	.0386	.0700	847
64.30	36.77	.005708	(.050)	(.120)	******	18.72	*****	.0209	.0396	.0291	.0532	724
66.70	41.47	.005778	(.040)	(.100)	******	18.61	*****	.0191	.0339	.0249	.0455	698
69.35	48.33	.005871	(.050)	(.090)	******	18.46	*****	.0106	.0267	.0193	.0353	632
71.70	54.57	.005748	(.040)	(.090)	******	18.65	*****	.0170	.0245	.0177	.0323	654
74.35	60.29	.005404	(.040)	(.100)	******	19.24	*****	.0036	.0262	.0191	.0347	777
76.70	62.13	.004910	(.050)	(.110)	******	20.18	*****	.0054	.0322	.0233	.0419	978

SCHUBAUER and KLEBANOFF 2100
nu = 0.000160 ft2/sec; fitted between y/delta = 0.15, 0.75 for x = 0.5 to 18.0 ft; fitted between y/delta = 0.15, 0.90 for x = 18.5 to 25.77 ft

ft	ft/sec		in.	in.	in.				in.	in.	in.	
.5	100.69	.003984	.04	.13	.2349	22.41	.413	.0016	.0390	.0274	.0486	1440
1.0	106.37	.003866	.08	.19	.3100	22.75	.325	.0012	.0462	.0333	.0593	1847
1.5	111.77	.003821	.08	.27	.3835	22.88	.223	.0049	.0518	.0383	.0687	2231
2.0	116.92	.003518	.08	.27	.3909	23.85	.410	.0066	.0592	.0432	.0770	2633
2.5	121.43	.003580	.08	.36	.4998	23.64	.221	.0055	.0642	.0480	.0860	3036
3.0	126.19	.003410	.08	.36	.4880	24.22	.345	.0041	.0681	.0506	.0904	3324
3.5	130.77	.003276	.13	.36	.5353	24.71	.392	.0031	.0752	.0558	.0997	3803
4.5	139.12	.003216	.13	.35	.5440	24.94	.404	.0030	.0768	.0573	.1024	4151
5.5	148.46	.003142	.13	.46	.6291	25.23	.365	.0045	.0846	.0639	.1145	4937
6.5	153.72	.002980	.13	.46	.7087	25.91	.440	.0027	.0989	.0748	.1336	5975
7.5	156.93	.002678	.19	.57	.8344	27.33	.666	.0008	.1274	.0945	.1678	7725
8.5	156.77	.002664	.19	.57	.8883	27.40	.651	.0018	.1337	.0993	.1765	8111
9.5	156.60	.002473	.19	.70	1.0682	28.44	.791	.0037	.1695	.1253	.2220	10221
10.5	158.07	.002522	.19	.84	1.2533	28.16	.644	.0020	.1804	.1353	.2409	11142
11.5	157.74	.002372	.27	.99	1.4552	29.04	.766	.0028	.2221	.1664	.2961	13674
12.5	158.15	.002450	.27	.99	1.4838	28.57	.652	.0012	.2184	.1662	.2976	13692

TABLE 1 (CONT'D)

x	U	Cf	ymin	ymax	delta	U/utau	PI	resid	displ	mom	energy	Rmom
13.5	158.39	.002429	.27	1.00	1.6164	28.69	.635	.0012	.2304	.1752	.3134	14456
14.5	159.36	.002388	.35	1.31	1.8460	28.94	.621	.0014	.2534	.1927	.3444	15906
15.5	159.04	.002332	.35	1.31	1.9725	29.29	.665	.0019	.2774	.2108	.3766	17462
16.5	159.28	.002355	.35	1.31	2.1478	29.14	.589	.0026	.2921	.2250	.4040	18662
17.5	160.00	.002325	.36	1.32	2.1169	29.33	.637	.0024	.2959	.2268	.4066	18904
18.0	159.04	.002361	.35	1.69	2.3178	29.11	.544	.0023	.3015	.2324	.4172	19247
18.5	157.26	.002302	.46	2.08	2.4292	29.48	.609	.0083	.3257	.2503	.4489	20500
19.0	154.05	.002184	.46	2.07	2.5798	30.40	.794	.0059	.3751	.2836	.5053	22755
19.5	150.94	.002112	.46	2.10	2.6117	30.77	.881	.0087	.3949	.2967	.5276	23326
20.0	147.69	.001989	.45	2.08	2.7033	31.71	1.082	.0066	.4376	.3221	.5681	24780
20.5	144.27	.001881	.54	2.47	3.0145	32.61	1.236	.0059	.5053	.3666	.6425	27546
21.0	141.04	.001754	.54	2.48	3.1327	33.77	1.485	.0071	.5618	.3983	.6921	29259
21.5	137.64	.001579	.54	2.47	3.2885	35.59	1.872	.0076	.6442	.4406	.7555	31587
22.0	133.58	.001463	.68	2.96	3.7164	36.97	2.127	.0094	.7679	.5181	.8845	36047
22.5	129.89	.001251	.68	3.49	4.3351	39.99	2.722	.0077	.9754	.6263	1.0493	42367
23.0	126.49	.001157	.68	3.50	4.4280	41.57	3.068	.0123	1.0626	.6732	1.1263	44351
23.5	122.79	.001020	.83	4.03	4.6454	44.27	3.645	.0100	1.1964	.7246	1.1953	46341
24.0	119.52	.000743	.83	4.57	5.3960	51.89	5.224	.0057	1.5818	.8721	1.3996	54291
24.5	116.37	.000592	1.17	5.11	5.8701	58.15	6.536	.0118	1.8636	.9693	1.5359	58746
25.0	113.93	.000312	1.16	6.09	7.1019	80.11	11.114	.0062	2.6172	1.1499	1.7570	68236
25.4	112.57	.000266	1.16	6.56	7.5077	86.73	12.489	.0119	2.8441	1.2076	1.8369	70801
25.77	111.77	.000113	1.57	7.79	8.7760	132.91	22.095	.0098	3.7203	1.3403	1.9998	78026

CLAUSER - flow 1 2200
nu = 0.000165 ft2/sec; fitted between y/delta = 0.125, 0.900

in.	ft/sec		in.	in.	in.				in.	in.	in.	
83	32.5	.002005	.40	2.00	2.471	30.90	1.719	.0016	.5387	.3406	.5025	5738
132	29.1	.001851	.50	3.00	3.976	32.88	1.973	.0036	.8794	.5644	.9503	8295
153	28.0	.001848	.60	4.00	4.602	32.90	1.925	.0026	.9999	.6464	1.0904	9141
223	25.2	.001911	.00	5.00	6.666	32.35	1.671	.0037	1.3443	.8990	1.5372	11442
286	23.6	.001905	1.25	7.00	8.770	32.40	1.577	.0060	1.7231	1.1773	2.0219	14032
323	22.5	.001823	1.50	9.00	10.134	33.12	1.688	.0043	2.0111	1.3639	2.3353	15499
357	21.8	.001887	1.50	10.00	11.164	32.55	1.530	.0048	2.1388	1.4705	2.5280	16191
387	21.2	.001819	2.00	10.00	12.204	33.16	1.633	.0023	2.3096	1.6236	2.7889	17384

CLAUSER - flow 2 2300
nu = 0.000165 ft2/sec; fitted between y/delta = 0.125, 0.900

in.	ft/sec		in.	in.	in.				in.	in.	in.	
90	26.1	.001246	.50	3.00	3.861	40.06	3.014	.0034	1.0903	.6105	.9881	8047
108	24.8	.001070	.75	4.00	4.715	43.24	4.230	.0092	1.3074	.7540	1.2066	9444
132	23.5	.001054	.75	5.00	5.903	43.56	4.214	.0031	1.7272	.9419	1.5105	11179
152	22.8	.001074	1.00	6.00	7.080	43.15	4.049	.0072	2.0257	1.1266	1.8163	12973
194	21.3	.001077	1.50	8.00	10.237	43.10	3.888	.0031	2.8506	1.6251	2.6364	17482
230	20.2	.000944	2.00	10.00	12.738	46.03	4.438	.0093	3.6829	2.0234	3.2400	20643
287	18.9	.000958	3.00	14.00	17.224	45.69	4.245	.0061	4.8044	2.7558	4.4584	26306
320	18.1	.000914	3.00	17.00	21.045	46.77	4.403	.0077	5.9730	3.3773	5.4589	30874

BRADSHAW and FERRISS, a = - 0.255 ---> 0 2400
nu = 0.000156 ft2/sec; outer fit for all stations
OUTER FIT DENOTED BY | |; INNER FIT DENOTED BY ( )

in.	ft/sec		in.	in.	in.				in.	in.	in.	
47	112.18	.001261	1.00	2.40	2.7435	33.83	2.977	.0017	.6079	.4132	.6853	24760
53	111.09	.001263	1.20	2.60	3.0574	30.79	2.920	.0014	.7330	.4572	.7604	27136
59	110.00	.001345	1.40	2.80	3.3107	38.56	2.617	.0013	.7541	.4831	.8098	28389
65	110.00	.001441	1.60	3.00	3.4510	37.25	2.310	.0007	.7417	.4877	.8247	28055
71	110.00	.001577	1.60	3.20	3.5908	35.61	1.932	.0007	.7177	.4877	.8341	28660
83	110.00	.001710	1.60	3.40	3.9279	34.20	1.578	.0008	.7211	.5060	.8763	29771
95	110.00	.001828	1.60	3.80	4.2397	33.08	1.293	.0011	.7174	.5183	.9060	30458
47	112.18	.001405	(.20)	(.40)	******	37.73	*****	.0020	.6569	.4136	.6889	24785
53	111.09	.001419	(.15)	(.30)	******	37.54	*****	.0015	.7196	.4578	.7649	27168
59	110.00	.001515	(.12)	(.25)	******	36.33	*****	.0037	.7427	.4842	.8152	28453
65	110.00	.001695	(.10)	(.20)	******	34.35	*****	.0036	.7232	.4881	.8313	28680
71	110.00	.001856	(.08)	(.15)	******	32.83	*****	.0020	.6987	.4869	.8383	28609
83	110.00	.002005	(.06)	(.15)	******	31.59	*****	.0014	.6920	.5006	.8735	29415
95	110.00	.002105	(.05)	(.15)	******	30.82	*****	.0017	.6888	.5108	.9001	30016

BRADSHAW, a = - 0.150 (probe displacement correction removed) 2500
nu = 0.0001562 ft2/sec; fitted between y/delta = 0.125, 0.900

in.	ft/sec		in.	in.	in.				in.	in.	in.	
24	143.42	.002210	.146	.796	1.0420	30.08	1.200	.0025	.1865	.1306	.2265	9993

TABLE 1 (CONT'D)

x	U	Cf	ymin	ymax	delta	U/utau	Pi	resid	displ	mom	energy	Rmom
48	129.22	.002127	.246	1.596	1.8379	30.66	1.098	.0014	.3095	.2231	.3906	15382
66	123.47	.002003	.296	1.996	2.3526	31.60	1.204	.0011	.4020	.2883	.5033	18994
84	118.98	.001905	.396	2.396	2.8384	32.40	1.306	.0012	.4944	.3530	.6146	22407

BRADSHAW and FERRISS, a = - 0.255 (flat pitot probe) 2600
nu = 0.0001562 ft2/sec: fitted between y/delta = 0.20, 0.90

in.	ft/sec		in.	in.	in.				in.	in.	in.	
23	136.51	.001239	.30	1.10	1.2644	40.17	3.342	.0040	.3351	.1964	.3210	14305
47	113.78	.001267	.60	2.40	2.7557	39.74	2.949	.0019	.6699	.4145	.6877	25165
65	104.93	.001289	.80	2.90	3.6101	39.38	2.777	.0038	.8474	.5356	.8943	29986
83	98.39	.001226	1.00	4.10	4.6767	40.39	2.899	.0024	1.1007	.6930	1.1539	36377

BRADSHAW, a = - 0.255 (round pitot probe; probe displacement correction removed) 2600a
nu = 0.0001562 ft2/sec; fitted between y/delta = 0.15, 0.90
sour point at x = 48, y = 2.196 suppressed in fitting

in.	ft/sec		in.	in.	in.				in.	in.	in.	
48	113.78	.001203	.496	2.196	2.6461	39.79	2.981	.0025	.6439	.3954	.6540	24000
84	98.39	.001197	.796	3.996	4.6446	40.88	3.008	.0020	1.1140	.6866	1.1586	36563

HERRING and NORBURY, beta = - 0.35 2700
nu = 0.000173 ft2/sec; fitted between y/delta = 0.15, 0.65

ft	ft/sec		in.	in.	in.				in.	in.	in.	
0	76.5	.003349	.15	.50	.8655	24.44	.397	.0017	.1248	.0923	.1645	3400
1	79.8	.003329	.15	.60	.9410	24.51	.352	.0024	.1297	.0966	.1726	3712
2	84.6	.003507	.15	.60	.9318	23.88	.185	.0049	.1159	.0882	.1591	3596
3	90.5	.003520	.15	.60	.9527	23.84	.130	.0016	.1123	.0861	.1555	3751
4	97.1	.003454	.15	.50	.8790	24.06	.186	.0011	.1107	.0849	.1535	3971
5	103.6	.003377	.15	.50	.8487	24.34	.233	.0013	.1123	.0863	.1562	4309

HERRING and NORBURY, beta = - 0.53 2800
nu = 0.000168 ft2/sec; fitted between y/delta = 0.15, 0.65

ft	ft/sec		in.	in.	in.				in.	in.	in.	
0	76.9	.003215	.20	.60	1.0705	24.94	.387	.0015	.1481	.1104	.1972	4211
1	82.6	.003285	.20	.70	1.1394	24.68	.261	.0027	.1438	.1091	.1960	4469
2	90.8	.003496	.20	.70	1.1399	23.92	.042	.0026	.1231	.0959	.1743	4318
3	101.4	.003691	.16	.60	.9552	23.28	-.069	.0010	.0956	.0752	.1375	3783
4	115.4	.003771	.13	.50	.8348	23.03	-.122	.0009	.0799	.0632	.1158	3617

PERRY 2900
nu = 0.000157 ft2/sec; fitted between y/delta = 0.125, 0.900 except incomplete last profile

ft	ft/sec		in.	in.	in.				in.	in.	in.	
2.5	122.09	.002013	.25	1.60	1.977	31.52	1.282	.0037	.3564	.2536	.4420	16434
4.0	109.18	.001737	.40	2.60	2.931	33.93	1.671	.0031	.5645	.3883	.6675	22505
5.5	100.98	.001458	.60	3.50	4.080	37.03	2.225	.0048	.8654	.5712	.9667	30615
7.0	92.96	.001117	.70	4.50	5.529	42.31	3.262	.0042	1.3598	.8374	1.3857	41316
8.5	88.68	.000917	.90	6.00	7.145	46.70	4.107	.0035	1.9070	1.1189	1.8242	52664
10.0	84.55	.000792	1.20	8.00	9.004	50.24	4.778	.0037	2.5323	1.4415	2.3317	64693
11.0	82.15	.000638	1.30	9.00	10.312	55.98	5.955	.0043	3.1322	1.6826	2.6791	73370
12.5	79.95	.000477	1.60	10.50	11.811	64.75	7.771	.0036	3.8985	1.9303	3.0139	81912
14.0	77.27	.000330	1.80	12.50	14.293	77.90	10.480	.0041	5.1278	2.3278	3.5696	95477
15.0	76.04	.000225	2.00	12.00	15.512	94.37	13.921	.0059	5.9811	2.4856	3.7603	100320

BELL - constant pressure 3000
nu = 0.000178 ft2/sec; fitted between y/delta = 0.15, 0.75 except as noted by * *

in.	ft/sec		in.	in.	in.				in.	in.	in.	
7.8	58.2	.004981	*.06*	.14	.1994	20.04	.282	.0025	.0341	.0224	.0392	610
10.5	58.2	.004463	.05	.18	.2637	21.17	.401	.0026	.0457	.0305	.0534	832
15.5	58.2	.004068	.06	.26	.3555	22.17	.481	.0024	.0608	.0411	.0719	1120
21.5	58.2	.003721	.08	.34	.4576	23.18	.584	.0023	.0792	.0540	.0943	1471
25.6	58.2	.003590	.08	.38	.5295	23.60	.606	.0015	.0909	.0625	.1091	1703
28.1	58.2	.003553	.10	.40	.5526	23.72	.612	.0014	.0934	.0640	.1117	1744
32.7	58.2	.003478	.10	.46	.6160	23.98	.616	.0025	.1043	.0723	.1266	1970
35.1	58.2	.003401	.10	.48	.6410	24.25	.656	.0025	.1093	.0753	.1318	2051
37.3	58.2	.003358	.12	.50	.6917	24.41	.653	.0025	.1180	.0823	.1440	2243

TABLE 1 (CONT'D)

x	U	Cf	ymin	ymax	delta	U/utau	Pi	resid	displ	mom	energy	Rmom
47.1	58.2	.003238	.15	.62	.8342	24.85	.660	.0016	.1387	.0974	.1705	2653
48.8	58.2	.003155	.15	.70	.9490	25.18	.669	.0016	.1565	.1106	.1939	3013
50.4	58.2	.003171	.20	.75	1.0205	25.11	.618	.0013	.1646	.1178	.2073	3208
BELL - flow D												3100
nu = 0.000178 ft2/sec; fitted between y/delta = 0.15, 0.60												
In.	ft/sec		In.	In.	In.				In.	In.	In.	
24.5	43.2	.004460	.10	.20	.4085	21.18	.333	.0013	.0667	.0453	.0795	916
28.4	44.1	.004303	.10	.25	.4608	21.56	.350	.0008	.0748	.0514	.0905	1061
32.6	45.3	.004166	.10	.30	.5147	21.91	.361	.0014	.0825	.0573	.1011	1215
36.9	46.2	.004115	.10	.30	.5588	22.05	.341	.0022	.0865	.0605	.1067	1308
40.8	46.7	.003994	.10	.35	.5971	22.38	.378	.0023	.0934	.0654	.1154	1431
49.5	49.2	.004004	.15	.40	.7169	22.35	.254	.0011	.1007	.0725	.1289	1670
54.5	50.2	.003940	.15	.40	.6950	22.53	.301	.0034	.1015	.0729	.1304	1712
59.8	52.0	.003882	.15	.45	.7633	22.70	.274	.0026	.1086	.0780	.1407	1921
BELL - flow F												3200
nu = 0.000178 ft2/sec; fitted between y/delta = 0.15, 0.90												
In.	ft/sec		In.	In.	In.				In.	In.	In.	
10.7	69.5	.003622	.10	.54	.6097	24.18	.376	.0039	.0992	.0697	.1224	2269
16.9	63.7	.002784	.14	.78	.8854	26.90	1.044	.0018	.1671	.1134	.1960	3383
22.8	60.1	.002521	.20	1.00	1.1134	28.17	1.242	.0034	.2195	.1474	.2532	4146
28.7	57.2	.002310	.25	1.20	1.3373	29.43	1.455	.0036	.2753	.1820	.3108	4875
39.3	52.5	.001958	.30	1.60	1.7961	31.96	1.913	.0031	.4032	.2575	.4339	6305
45.1	50.6	.001843	.40	1.80	2.0318	32.94	2.084	.0035	.4676	.2951	.4951	6991
50.8	48.7	.001610	.40	2.00	2.3212	35.24	2.542	.0047	.5749	.3509	.5822	8000
56.9	46.8	.001372	.50	2.40	2.7255	38.18	3.125	.0046	.7240	.4240	.6946	9289
BRADSHAW - layer C (probe displacement correction removed)												3300
nu = 0.0001562 ft2/sec; fitted between y/delta = 0.10, 0.90												
In.	ft/sec		In.	In.	In.				In.	In.	In.	
24	125.63	.002558	.246	.996	1.1439	27.96	.749	.0018	.1760	.1291	.2282	8656
30	120.48	.002449	.146	1.196	1.3629	28.58	.826	.0012	.2108	.1540	.2716	9901
36	116.85	.002187	.196	1.346	1.5476	30.24	1.149	.0029	.2700	.1920	.3346	11765
42	110.76	.002015	.196	1.546	1.7571	31.51	1.384	.0030	.3262	.2263	.3921	13370
48	107.13	.001922	.196	1.746	1.9624	32.26	1.515	.0037	.3717	.2552	.4398	14587
60	101.40	.001713	.246	2.096	2.3650	34.17	1.886	.0024	.4863	.3268	.5560	17678
72	96.82	.001578	.296	2.496	2.7793	35.60	2.122	.0017	.5980	.3923	.6629	20263
84	92.95	.001510	.396	2.846	3.1858	36.39	2.248	.0018	.6968	.4527	.7700	22448
NEWMAN (corrected for turbulence)												3500
nu = 0.000156 ft2/sec; fitted between y/delta = 0.15, 0.90												
In.	ft/sec		In.	In.	In.				In.	In.	In.	
24.11	152.6	.001739	.10	.35	.4370	33.91	2.448	.0046	.1095	.0660	.1093	5378
33.11	134.9	.001413	.15	.75	.8408	37.62	2.994	.0037	.2185	.1288	.2110	9283
42.11	119.4	.001104	.20	1.15	1.3280	42.57	3.903	.0033	.3735	.2095	.3380	13360
48.11	111.6	.000916	.30	1.60	1.8033	46.73	4.684	.0031	.5363	.2898	.4636	17278
54.11	103.9	.000758	.40	2.10	2.3510	51.37	5.586	.0023	.7367	.3822	.6047	21211
57.11	100.8	.000530	.50	2.40	2.7266	61.42	7.677	.0046	.9418	.4466	.6940	24050
59.11	99.6	.000318	.50	2.80	3.1289	79.30	11.407	.0058	1.1975	.5062	.7703	26932
NEWMAN (turbulence correction removed)												3500a
nu = 0.000156 ft2/sec; fitted between y/delta = 0.15, 0.90												
In.	ft/sec		In.	In.	In.				In.	In.	In.	
24.11	152.6	.001775	.10	.35	.4366	33.56	2.372	.0046	.1081	.0656	.1088	5346
33.11	134.9	.001453	.15	.75	.8383	37.10	2.883	.0036	.2148	.1277	.2098	9205
42.11	119.4	.001143	.20	1.15	1.3236	41.83	3.745	.0031	.3667	.2080	.3367	13270
48.11	111.6	.000955	.30	1.60	1.7966	45.77	4.478	.0030	.5260	.2879	.4618	17162
54.11	103.9	.000806	.40	2.10	2.3423	49.80	5.251	.0024	.7186	.3794	.6029	21056
57.11	100.8	.000592	.50	2.40	2.7174	58.13	6.978	.0042	.9120	.4449	.6951	23959
59.11	99.6	.000375	.50	2.80	3.1212	73.00	10.076	.0054	1.1588	.5085	.7781	27053

TABLE 1 (CONT'D)

x	U	Cf	ymin	ymax	delta	U/utau	PI	resid	displ	mom	energy	Rmom
MENDELSOHN - basic flap contour, 0 degrees (figures 15, 21)												4200
nu = 0.0001578 ft2/sec; fitted between y/delta = 0.10, 0.90 except as noted by * *												
trailing edge is at x = 48 in.												
in.	ft/sec		in.	in.	in.				in.	in.	in.	
8.06	164.1	.003683	.048	.105	.1529	23.30	.581	.0036	.0258	.0178	.0314	1545
14.40	166.5	.003168	.027	.206	.2429	25.13	.753	.0087	.0407	.0286	.0501	2511
19.20	170.3	.003159	.029	.202	.2859	25.16	.668	.0095	.0468	.0332	.0583	2983
21.60	170.0	.003107	.048	.212	.2912	25.57	.707	.0045	.0485	.0343	.0603	3081
24.00	168.9	.002891	.042	.278	.3398	26.30	.842	.0097	.0595	.0416	.0725	3705
27.60	166.7	.002760	.071	.274	.3938	26.92	.913	.0003	.0710	.0499	.0872	4390
37.20	152.2	.002246	.091	.432	.6060	29.84	1.394	.0126	.1175	.0791	.1357	6355
38.40	150.7	.001984	.070	.521	.6443	31.75	1.791	.0091	.1386	.0905	.1537	7200
39.65	147.7	.001962	.139	.444	.7069	31.93	1.795	.0077	.1474	.0953	.1608	7430
43.20	138.8	.001675	.137	.590	.8132	34.56	2.333	.0070	.1906	.1187	.1980	8703
46.94	136.5	.001557	.144	.790	.9945	35.85	2.523	.0076	.2413	.1503	.2508	10828
48.00	136.6	.001564	.127	.835	1.0080	35.77	2.498	.0069	.2432	.1507	.2508	10873
WAKE FITTED TO WALL-WAKE FORMULA												
48.62	137.7	.001814	.166	.871	1.0881	33.20	1.893	.0028	.2324	.1526	.2582	11078
49.20	138.7	.001949	.151	.912	1.0646	32.04	1.644	.0035	.2144	.1435	.2449	10510
50.40	140.1	.002081	.122	.893	1.0336	31.00	1.425	.0082	.1989	.1341	.2301	9920
52.80	141.6	.002407	.168	.598	1.0691	28.83	.920	.0082	.1724	.1241	.2173	9273
WAKE FITTED TO WAKE FORMULA ALONE												
48.62	137.7	*******	*.322*	.871	1.0998	*****	*****	.0015	.2253	.1533	.2610	11145
49.20	138.7	*******	*.293*	.912	1.0544	*****	*****	.0028	.2051	.1439	.2474	10539
50.40	140.1	*******	*.285*	.893	1.0092	*****	*****	.0043	.1859	.1338	.2320	9900
52.80	141.6	*******	*.329*	*.965*	1.0067	*****	*****	.0048	.1579	.1217	.2165	9096
SCHUBAUER and SPANGENBERG - distribution A												4400
nu = 0.000168 ft2/sec; fitted between y/delta = 0.15, 0.90												
in.	ft/sec		in.	in.	in.				in.	in.	in.	
-10	82.10	.003312	.150	.550	.6999	24.57	.484	.0012	.1048	.0758	.1342	3088
0	80.34	.003118	.150	.750	.8355	25.33	.577	.0012	.1288	.0930	.1642	3706
10	79.45	.003012	.150	.850	.9040	25.77	.599	.0025	.1512	.1096	.1936	4321
20	76.30	.002835	.250	.950	1.1620	26.56	.714	.0019	.1849	.1333	.2347	5045
30	72.80	.002390	.225	1.125	1.3986	28.93	1.172	.0025	.2599	.1799	.3116	6497
40	69.01	.001992	.375	1.425	1.7240	31.69	1.706	.0032	.3632	.2401	.4087	8219
50	63.02	.001468	.500	1.900	2.3103	36.91	2.751	.0050	.5796	.3536	.5861	11052
SCHUBAUER and SPANGENBERG - distribution B												4500
nu = 0.000165 ft2/sec; fitted between y/delta = 0.15, 0.90												
in.	ft/sec		in.	in.	in.				in.	in.	in.	
0	81.81	.003023	.150	.750	.8724	25.72	.625	.0011	.1363	.0982	.1732	4059
20	79.25	.002741	.250	1.050	1.2026	27.01	.769	.0014	.1939	.1394	.2450	5580
40	74.31	.002500	.375	1.425	1.6422	28.29	.930	.0025	.2769	.1984	.3475	7444
60	67.50	.001935	.375	2.025	2.3609	32.15	1.653	.0052	.4813	.3243	.5553	11057
80	61.04	.001374	.500	2.900	3.2554	38.15	2.858	.0040	.8054	.4919	.8140	15164
100	54.61	.000979	.750	3.750	4.4827	45.20	4.285	.0032	1.2768	.7108	1.1442	19605
120	50.47	.000420	1.000	5.800	6.5343	69.03	9.232	.0058	2.3591	1.0604	1.6279	27030
SCHUBAUER and SPANGENBERG - distribution C												4600
nu = 0.000168 ft2/sec; fitted between y/delta = 0.15, 0.90												
in.	ft/sec		in.	in.	in.				in.	in.	in.	
0	79.95	.003212	.150	.650	.8022	24.96	.515	.0009	.1207	.0876	.1549	3473
20	77.84	.002925	.250	.950	1.1334	26.15	.625	.0007	.1743	.1270	.2244	4903
40	75.47	.002728	.250	1.350	1.5298	27.08	.699	.0019	.2364	.1727	.3052	6665
60	70.60	.002243	.375	1.875	2.1971	29.86	1.170	.0041	.3934	.2772	.4824	9709
80	64.26	.001858	.625	2.375	2.8408	32.81	1.740	.0035	.5805	.3886	.6631	12388
100	59.93	.001526	.750	2.750	3.5920	36.20	2.407	.0025	.8241	.5236	.8773	15568
120	55.33	.001164	.750	3.750	4.4512	41.45	3.477	.0036	1.1714	.6873	1.1224	18865
140	51.33	.001016	1.250	4.750	5.3761	44.36	4.051	.0038	1.4917	.8463	1.3685	21547
160	47.57	.000827	1.250	5.750	6.8999	49.18	5.004	.0098	2.0567	1.1106	1.7730	26203
180	47.06	.000761	1.500	7.500	8.7492	51.25	5.336	.0041	2.6440	1.4200	2.2650	33149
200	43.57	.000193	2.500	10.500	12.0766	101.74	15.908	.0058	4.9070	1.9063	2.8717	41202

TABLE 1 (CONT'D)

x	U	Cf	ymin	ymax	delta	U/utau	PI	resid	displ	mom	energy	Rmom
SCHUBAUER and SPANGENBERG - distribution D												4700
nu = 0.000168 ft2/sec; fitted between y/delta = 0.15, 0.90												
in.	ft/sec		in.	in.	in.				in.	in.	in.	
0	80.83	.003269	.150	.650	.8036	24.74	.460	.0004	.1178	.0861	.1528	3451
30	69.01	.002203	.225	1.275	1.4662	30.13	1.443	.0053	.2920	.1964	.3366	6723
60	57.50	.001067	.625	2.625	3.0884	43.30	4.043	.0049	.8874	.4983	.8069	14215
90	49.44	.000730	1.000	4.200	4.8347	52.34	5.841	.0055	1.5387	.7829	1.2321	19200
115	44.91	.000369	1.400	6.600	7.4046	73.59	10.203	.0061	2.7519	1.1995	1.8335	26723
SCHUBAUER and SPANGENBERG - distribution F												4800
nu = 0.000170 ft2/sec; fitted between y/delta = 0.15, 0.90												
in.	ft/sec		in.	in.	in.				in.	in.	in.	
0	81.71	.003311	.150	.650	.7909	24.58	.433	.0015	.1145	.0838	.1488	3356
30	78.75	.002875	.225	.975	1.1909	26.38	.651	.0017	.1842	.1340	.2367	5173
60	74.84	.002486	.300	1.500	1.8440	28.37	.901	.0015	.3075	.2219	.3899	8142
100	67.27	.002023	.500	2.500	2.8232	31.45	1.425	.0024	.5321	.3665	.6314	12087
140	59.13	.001565	.750	3.450	3.9663	35.75	2.265	.0023	.8862	.5705	.9594	16537
160	54.78	.001429	.750	4.250	4.9784	37.41	2.555	.0034	1.1607	.7362	1.2326	19761
180	50.63	.001009	1.500	5.700	6.6320	44.53	3.996	.0052	1.8145	1.0436	1.6947	25900
190	48.72	.000606	1.200	6.800	7.8225	57.44	6.707	.0098	2.5626	1.2866	2.0231	30723
200	45.18	.000336	2.500	8.500	10.1995	77.12	10.794	.0033	3.8089	1.6495	2.5162	36530
200	47.57	.000334	2.500	9.500	10.5834	77.42	10.812	.0116	3.9217	1.7105	2.6127	39882
SCHUBAUER and SPANGENBERG - distribution F												4900
nu = 0.000169 ft2/sec; fitted between y/delta = 0.15, 0.90												
in.	ft/sec		in.	in.	in.				in.	in.	in.	
0	81.81	.003314	.150	.650	.7993	24.57	.421	.0013	.1148	.0842	.1496	3397
50	76.20	.002717	.375	1.275	1.5266	27.13	.709	.0021	.2373	.1732	.3057	6506
120	66.91	.002066	.500	2.500	2.9759	31.11	1.324	.0018	.5433	.3787	.6550	12495
160	63.14	.001873	.900	3.300	4.1741	32.68	1.531	.0029	.7957	.5521	.9533	17189
190	55.04	.001402	1.200	5.200	6.1915	37.77	2.518	.0019	1.4116	.9052	1.5195	24569
210	51.40	.000817	2.000	6.800	8.1270	49.49	4.954	.0036	2.3851	1.3076	2.0954	33144
220	47.75	.000409	1.500	8.500	9.9539	69.92	9.249	.0124	3.5581	1.6357	2.5292	38493
STRATFORD - experiment 5												5200
nu = 0.000157 ft2/sec; fitted between y/delta = 0.15, 0.90 except as noted												
OUTER FIT DENOTED BY | | ; INNER FIT DENOTED BY ( )												
in.	ft/sec		in.	in.	in.				in.	in.	in.	
34.89	55.00	.003575	.15	.60	.7337	23.65	.419	.0014	.1110	.0800	.1419	2337
35.99	52.06	.003186	|.30|	.70	.8110	25.06	.713	.0025	.1382	.0965	.1689	2668
36.45	49.83	.002759	|.30|	.80	.9071	26.93	1.098	.0039	.1757	.1182	.2037	3127
42.37	44.07	.001467	|.50|	1.10	1.2325	36.93	3.215	.0059	.3454	.1938	.3149	4533
49.24	42.03	.001297	.30	1.20	1.4939	39.27	3.653	.0022	.4369	.2384	.3841	5318
63.86	37.06	.001286	.40	1.80	2.1938	39.44	3.561	.0048	.6233	.3461	.5589	6809
74.83	34.08	.001059	.50	2.50	2.9811	43.46	4.323	.0065	.8978	.4805	.7680	8692
42.37	44.07	.001194	(.10)	(.15)	******	40.93	******	.0007	.3682	.1923	.3081	4499
STRATFORD - experiment 6												5300
nu = 0.000157 ft2/sec; fitted between y/delta = 0.15, 0.90 except as noted												
OUTER FIT DENOTED BY | | ; INNER FIT DENOTED BY ( )												
in.	ft/sec		in.	in.	in.				in.	in.	in.	
34.89	55.00	.003599	.15	.60	.7304	23.57	.404	.0031	.1095	.0790	.1401	2306
35.99	51.54	.003187	|.30|	.70	.8509	25.05	.693	.0014	.1432	.1005	.1760	2749
36.45	49.19	.002565	|.30|	.80	.9071	27.92	1.327	.0052	.1880	.1236	.2113	3227
42.37	42.64	.000633	|.50|	1.10	1.3224	56.19	7.355	.0055	.4834	.2151	.3325	4867
49.24	39.32	.000500	.30	1.70	1.9065	63.27	8.724	.0086	.7177	.3048	.4660	6361
63.86	33.73	.000275	.60	3.00	3.5223	85.24	13.146	.0121	1.4276	.5448	.8179	9753
74.83	31.02	.000262	.80	4.00	4.6957	87.40	13.500	.0157	1.9085	.7353	1.1108	12105
42.37	42.64	.000558	(.15)	(.15)	******	59.85	******	.0000	.4972	.2108	.3243	4771
KLEBANOFF and DIEHL - free transition												5400
nu = 0.000178 ft2/sec; fitted between y/delta = 0.15, 0.75												
ft	ft/sec		in.	in.	in.				in.	in.	in.	
7.50	107.5	.003007	.135	.588	.8331	25.79	.565	.0019	.1247	.0911	.1613	4585
8.50	107.5	.002817	.160	.672	1.0038	26.65	.664	.0024	.1552	.1132	.2001	5699

TABLE 1 (CONT'D)

x	U	cf	ymin	ymax	delta	U/utau	Pi	resid	displ	mom	energy	Rmom
9.50	107.5	.002728	.194	.804	1.1482	27.08	.693	.0020	.1780	.1303	.2302	6556
10.50	107.5	.002657	.211	.959	1.3424	27.44	.695	.0017	.2050	.1509	.2672	7597

KLEBANOFF and DIEHL - 0.04-inch rod 5500
nu = 0.000174 ft2/sec; fitted between y/delta = 0.15, 0.75 except as noted by * *

ft	ft/sec		in.	in.	in.				in.	in.	in.	
4.17	107.4	.003611	.042	.140	.2045	23.54	.748	.0020	.0393	.0262	.0454	1346
4.67	107.4	.003554	*.122*	.280	.3889	23.72	.469	.0027	.0602	.0429	.0757	2207
5.17	107.4	.003480	.092	.328	.4849	23.97	.416	.0020	.0724	.0528	.0938	2714
6.00	107.4	.003203	.133	.487	.6557	24.99	.494	.0012	.0975	.0712	.1264	3665
7.50	107.4	.002968	.133	.606	.8393	25.96	.588	.0019	.1274	.0931	.1649	4787
10.50	107.4	.002584	.213	1.040	1.4192	27.82	.742	.0014	.2197	.1613	.2852	8298

KLEBANOFF and DIEHL - 0.25-inch rod 5600
nu = 0.000174 ft2/sec; fitted between y/delta = 0.15, 0.75 except as noted
OUTER FIT DENOTED BY | |; INNER FIT DENOTED BY ( )

ft	ft/sec		in.	in.	in.				in.	in.	in.	
4.17	113.9	.000016	|.217|	.473	.6338	356.55	69.781	.0064	.3078	.0823	.1230	4487
4.25	109.2	.000808	|.250|	.506	.6774	49.77	5.893	.0026	.2315	.1117	.1751	5842
4.67	107.4	.002996	|.309|	.683	1.0110	25.84	.468	.0009	.1430	.1069	.1908	5499
5.17	107.6	.003184	|.411|	.804	1.1686	25.06	.220	.0018	.1418	.1094	.1978	5639
6.00	107.2	.003255	|.414|	1.201	1.6804	24.79	-.021	.0021	.1620	.1298	.2374	6664
7.50	107.2	.003095	.330	1.432	1.9628	25.42	.044	.0014	.1995	.1590	.2906	8165
8.50	107.2	.002973	.389	1.590	2.2102	25.94	.100	.0010	.2319	.1845	.3366	9474
9.50	107.2	.002854	.349	1.707	2.3069	26.47	.199	.0021	.2606	.2064	.3751	10598
10.50	107.2	.002747	.406	1.784	2.4285	26.98	.288	.0027	.2905	.2285	.4147	11733
4.17	113.9	.000213	(.099)	(.099)	******	96.79	******	.0000	.2963	.0913	.1340	4983
4.25	109.2	.001200	(.053)	(.093)	******	40.83	******	.0013	.2232	.1145	.1807	5987
4.67	107.4	.003360	(.093)	(.171)	******	24.40	******	.0129	.1344	.1035	.1867	5326
5.17	107.6	.003519	(.096)	(.194)	******	23.84	******	.0131	.1319	.1047	.1912	5395
6.00	107.2	.003388	(.138)	(.256)	******	24.30	******	.0072	.1578	.1271	.2335	6527

KLEBANOFF and DIEHL - 24 mesh screen 5700
nu = 0.000170 ft2/sec; fitted between y/delta = 0.15, 0.75

ft	ft/sec		in.	in.	in.				in.	in.	in.	
2.00	43.4	.002816	.231	.723	1.0910	26.05	1.054	.0027	.2074	.1390	.2389	2956
3.50	43.4	.003202	.290	1.156	1.5321	24.99	.512	.0020	.2291	.1663	.2942	3538
4.50	43.4	.003229	.272	1.296	1.7574	24.89	.420	.0032	.2465	.1818	.3233	3867
6.50	43.4	.003083	.411	1.395	2.1143	25.47	.458	.0007	.2999	.2226	.3967	4737
10.50	43.4	.002890	.511	1.988	2.8281	26.31	.500	.0033	.3964	.2960	.5276	6298

KLEBANOFF and DIEHL - sandpaper, 35 ft/sec 5800
nu = 0.000165 ft2/sec; fitted between y/delta = 0.15, 0.75 except as noted
OUTER FIT DENOTED BY | |; INNER FIT DENOTED BY ( )

ft	ft/sec		in.	in.	in.				in.	in.	in.	
2.08	35.5	.002179	|.310|	.704	1.0127	30.29	1.087	.0062	.2481	.1497	.2492	2683
2.50	35.5	.002378	|.309|	.703	1.1223	29.00	1.650	.0010	.2544	.1594	.2682	2858
3.00	35.5	.002724	|.308|	.800	1.2783	27.10	1.160	.0043	.2504	.1656	.2834	2969
4.00	35.5	.003019	.307	1.095	1.5320	25.74	.765	.0032	.2591	.1811	.3160	3246
5.00	35.5	.003063	.309	1.294	1.7447	25.55	.658	.0022	.2800	.1998	.3513	3583
5.50	35.5	.003049	.308	1.391	1.8907	25.61	.632	.0024	.2947	.2112	.3715	3786
6.50	35.5	.003069	.406	1.391	2.1018	25.53	.560	.0018	.3174	.2311	.4090	4143
7.50	35.5	.002981	.406	1.587	2.1898	25.90	.623	.0016	.3405	.2472	.4365	4432
8.50	35.5	.002959	.405	1.684	2.3702	26.00	.605	.0041	.3628	.2642	.4675	4737
9.50	35.5	.002941	.408	1.687	2.5701	26.08	.582	.0016	.3858	.2829	.5011	5073
10.50	35.5	.002887	.603	1.981	2.7452	26.32	.604	.0024	.4138	.3037	.5381	5445
2.08	35.5	.001852	(.113)	(.113)	******	32.87	*****	.0000	.2581	.1493	.2465	2676
2.50	35.5	.002570	(.112)	(.152)	******	27.90	*****	.0028	.2506	.1593	.2690	2857
3.00	35.5	.002878	(.111)	(.151)	******	26.36	*****	.0008	.2473	.1653	.2837	2954

KLEBANOFF and DIEHL - sandpaper, 55 ft/sec 5900
nu = 0.000166 ft2/sec; fitted between y/delta = 0.15, 0.75 except as noted
OUTER FIT DENOTED BY | |; INNER FIT DENOTED BY ( )

ft	ft/sec		in.	in.	in.				in.	in.	in.	
2.08	55.1	.001858	|.310|	.704	.9905	32.81	2.336	.0036	.2485	.1490	.2468	4122
2.50	55.1	.002089	|.308|	.702	1.1324	30.94	1.858	.0014	.2559	.1606	.2692	4442
3.00	55.1	.002465	|.310|	.802	1.2962	28.48	1.245	.0019	.2490	.1671	.2864	4621

TABLE I (CONT'D)

x	U	Cf	ymin	ymax	delta	U/utau	PI	resid	displ	mom	energy	Rmom
4.00	55.1	.002695	.310	1.098	1.5839	27.24	.868	.0020	.2669	.1889	.3300	5224
5.00	55.1	.002809	.326	1.192	1.7695	26.69	.686	.0013	.2763	.2006	.3537	5548
5.50	55.1	.002837	.310	1.196	1.8390	26.55	.639	.0033	.2814	.2060	.3644	5697
6.50	55.1	.002840	.406	1.391	2.1266	26.54	.563	.0008	.3065	.2268	.4025	6273
7.50	55.1	.002843	.406	1.587	2.2401	26.53	.535	.0014	.3183	.2368	.4210	6550
8.50	55.1	.002782	.405	1.684	2.4299	26.81	.559	.0021	.3481	.2595	.4618	7179
9.50	55.1	.002760	.406	1.685	2.6130	26.92	.545	.0010	.3705	.2774	.4943	7672
10.50	55.1	.002726	.427	1.884	2.7348	27.09	.560	.0019	.3835	.2919	.5202	8074
2.08	55.1	.001594	(.074)	(.113)	******	35.42	*****	.0024	.2581	.1486	.2441	4111
2.50	55.1	.002303	(.111)	(.151)	******	29.47	*****	.0003	.2512	.1605	.2702	4439
3.00	55.1	.002663	(.113)	(.153)	******	27.41	*****	.0020	.2445	.1665	.2805	4606

KLEBANOFF and DIEHL - sandpaper, 108 ft/sec 6000
nu = 0.000165 ft2/sec; fitted between y/delta = 0.15, 0.75 except as noted
OUTER FIT DENOTED BY | |; INNER FIT DENOTED BY ( )

ft	ft/sec		in.	in.	in.				in.	in.	in.	
2.08	108.5	.001664	|.340|	.734	1.0034	34.67	2.397	.0013	.2415	.1496	.2492	8197
2.50	108.5	.001896	|.242|	.734	1.1261	32.48	1.858	.0016	.2428	.1580	.2672	8658
3.00	108.5	.002190	|.340|	.832	1.3092	30.22	1.283	.0022	.2407	.1642	.2867	9106
4.00	108.5	.002472	.240	1.126	1.5885	28.44	.703	.0020	.2452	.1706	.3167	9841
5.00	108.5	.002550	.305	1.191	1.8181	28.00	.627	.0010	.2586	.1937	.3444	10613
5.50	108.5	.002561	.340	1.325	1.8913	27.95	.595	.0040	.2653	.2001	.3565	10964
6.50	108.5	.002564	.338	1.421	2.1078	27.93	.537	.0019	.2845	.2161	.3865	11843
7.50	108.5	.002550	.404	1.586	2.2581	28.00	.519	.0011	.3008	.2295	.4112	12577
8.50	108.5	.002543	.435	1.616	2.4571	28.04	.480	.0013	.3188	.2448	.4394	13414
9.50	108.5	.002492	.404	1.880	2.5958	28.33	.522	.0022	.3436	.2637	.4730	14452
10.50	108.5	.002475	.503	1.892	2.7449	28.43	.516	.0006	.3603	.2769	.4975	15171
2.08	108.5	.001320	(.065)	(.084)	******	38.72	*****	.0005	.2560	.1404	.2457	8185
2.50	108.5	.002049	(.104)	(.143)	******	31.24	*****	.0014	.2395	.1579	.2677	8651
3.00	108.5	.002341	(.084)	(.143)	******	29.23	*****	.0006	.2364	.1654	.2864	9064

BAUER - 20 degree slope 6100
nu = 0.00000944 ft2/sec; fitted between y/delta = 0.15, 0.60 except as noted by * *

ft	ft/sec		in.	in.	in.				in.	in.	in.	
3	8.34	.004024	*.120*	*.192*	.2771	22.29	.135	.0012	.0372	.0279	.0504	2056
4	9.68	.003533	*.096*	*.240*	.3994	23.79	.218	.0049	.0515	.0389	.0700	3324
5	10.89	.003475	.072	.192	.4709	23.99	.241	.0018	.0501	.0382	.0689	3673
6	12.06	.003215	.096	.288	.4975	24.94	.268	.0024	.0620	.0474	.0853	5040
7	12.85	.003128	.096	.288	.5194	25.29	.282	.0017	.0669	.0514	.0928	5829
8	13.69	.003001	.096	.288	.5709	25.82	.314	.0015	.0758	.0587	.1060	7087
9	14.51	.002927	.096	.336	.6323	26.14	.314	.0010	.0815	.0634	.1146	8117
10	15.26	.002847	.120	.432	.7255	26.51	.302	.0023	.0902	.0704	.1275	9486
11	15.97	.002736	.120	.432	.7498	27.04	.382	.0022	.0945	.0737	.1405	10949
12	16.68	.002711	.144	.540	.8980	27.16	.298	.0016	.1080	.0850	.1542	12515
13	17.31	.002681	.144	.540	.9360	27.31	.292	.0026	.1127	.0891	.1620	13617
14	17.97	.002640	.168	.600	1.0164	27.48	.269	.0018	.1176	.0933	.1698	14805
15	18.58	.002604	.192	.600	1.1786	27.71	.231	.0015	.1208	.1024	.1865	16795
16	19.17	.002573	.192	.600	1.1496	27.88	.265	.0024	.1290	.1025	.1864	17340

BAUER - 40 degree slope 6200
nu = 0.00001052 ft2/sec; fitted between y/delta = 0.15, 0.60 except as noted by * *

ft	ft/sec		in.	in.	in.				in.	in.	in.	
2	10.77	.004075	*.084*	.144	.2619	22.16	.059	.0007	.0314	.0235	.0423	2003
3	12.60	.003800	*.108*	.192	.3375	22.94	.032	.0018	.0382	.0293	.0532	2927
4	14.10	.003605	*.072*	.216	.3903	23.56	.042	.0022	.0431	.0334	.0606	3727
5	15.55	.003358	.072	.240	.4587	24.48	.121	.0025	.0520	.0403	.0731	4969
6	16.84	.003094	.084	.276	.4982	25.43	.252	.0025	.0614	.0474	.0857	6328
7	18.02	.002992	.096	.348	.6013	25.86	.222	.0010	.0701	.0546	.0988	7791
8	19.12	.002912	.096	.348	.6316	26.21	.246	.0016	.0753	.0589	.1067	8923
9	20.19	.002829	.120	.420	.7256	26.59	.235	.0019	.0831	.0652	.1184	10431
10	21.20	.002753	.120	.420	.7656	26.95	.265	.0017	.0900	.0709	.1288	11913
11	22.09	.002686	.144	.468	.8155	27.29	.288	.0021	.0954	.0750	.1361	13131
12	23.08	.002633	.144	.516	.9261	27.50	.263	.0011	.1048	.0830	.1508	15170
13	23.95	.002593	.168	.564	1.0073	27.77	.250	.0014	.1113	.0884	.1609	16778
14	24.79	.002543	.168	.612	1.0654	28.05	.206	.0011	.1199	.0956	.1742	18783

BAUER - 60 degree slope 6300
nu = 0.00000974 ft2/sec; fitted between y/delta = 0.15, 0.60

ft	ft/sec		in.	in.	in.				in.	in.	in.	
2	13.88	.003165	.048	.168	.3009	25.14	.499	.0012	.0461	.0341	.0607	4046

TABLE 1 (CONT'D)

x	U	Cf	ymin	ymax	delta	U/utau	PI	resid	displ	mom	energy	Rmom
3	15.83	.003044	.072	.240	.4090	25.63	.390	.0011	.0550	.0415	.0743	5621
4	17.52	.003027	.072	.240	.4366	25.70	.323	.0012	.0573	.0441	.0796	6611
5	18.98	.002934	.084	.288	.4947	26.11	.312	.0015	.0623	.0482	.0870	7826
6	20.47	.002831	.096	.336	.5716	26.58	.307	.0007	.0703	.0548	.0991	9592
7	21.78	.002754	.096	.336	.6075	26.95	.327	.0016	.0759	.0594	.1076	11072
8	23.02	.002664	.108	.384	.6769	27.40	.347	.0016	.0838	.0657	.1189	12933
9	24.19	.002634	.120	.432	.7514	27.55	.304	.0017	.0894	.0707	.1283	14624
10	25.34	.002592	.144	.480	.8339	27.78	.279	.0013	.0976	.0778	.1417	16860
11	26.39	.002549	.144	.480	.8682	28.01	.290	.0015	.1004	.0798	.1452	18021
12	27.45	.002510	.144	.540	.9508	28.23	.274	.0014	.1079	.0863	.1573	20263

BRADSHAW - layer A (probe displacement correction removed) 6400
nu = 0.0001585 ft2/sec; fitted between y/delta = 0.10, 0.90
sour point at x = 72, y = 0.996 suppressed in fitting

in.	ft/sec		in.	in.	in.				in.	in.	in.	
24	125.63	.002979	.051	.396	.4668	25.91	.746	.0018	.0780	.0551	.0966	3640
30	120.48	.002647	.076	.496	.5846	27.49	1.007	.0022	.1057	.0733	.1273	4644
36	114.85	.002317	.106	.646	.7668	29.38	1.317	.0020	.1489	.1011	.1738	6103
42	110.76	.002110	.106	.796	.9347	30.79	1.548	.0013	.1901	.1268	.2165	7383
48	107.13	.002135	.106	.896	1.0392	30.61	1.472	.0047	.2068	.1394	.2388	7852
60	101.40	.002034	.146	1.196	1.3727	31.36	1.526	.0022	.2712	.1837	.3146	9793
72	96.82	.001923	.196	1.546	1.7480	32.25	1.625	.0016	.3515	.2379	.4064	12110
84	92.95	.001849	.246	1.896	2.1523	32.89	1.682	.0024	.4304	.2911	.4977	14225

BRADSHAW - layer B (probe displacement correction removed) 6500
nu = 0.0001562 ft2/sec; fitted between y/delta = 0.10, 0.90
sour point at x = 48, y = 0.996 suppressed in fitting

in.	ft/sec		in.	in.	in.				in.	in.	in.	
24	125.63	.002686	.076	.646	.7196	27.29	.830	.0035	.1188	.0848	.1484	5682
30	120.48	.002510	.106	.796	.8956	28.23	.952	.0013	.1528	.1085	.1895	6976
36	114.85	.002233	.146	.946	1.0661	29.03	1.267	.0022	.1985	.1373	.2375	8413
42	110.76	.002051	.146	1.096	1.2583	31.23	1.489	.0021	.2463	.1675	.2874	9899
48	107.13	.001968	.146	1.196	1.4311	31.88	1.585	.0019	.2827	.1907	.3264	10902
60	101.40	.001818	.196	1.596	1.8229	33.16	1.775	.0027	.3731	.2492	.4248	13482
72	96.82	.001685	.246	1.946	2.2031	34.45	1.986	.0022	.4670	.3082	.5224	15919
84	92.95	.001652	.296	2.296	2.5996	34.79	1.998	.0028	.5500	.3632	.6172	18010

Notes for figure 1:

(a) flow 1600 (Riabouchinsky 1914); last 5 profiles; complete profiles are at x = 4, 10.94 m.

(b) flow 2200 (Clauser 1954, flow 1); 8 profiles, renormalized; complete profiles are at x = 83, 327 in.

(c) flow 2500 (Bradshaw 1966, a = -0.150); round pitot tube (displacement correction removed); 4 profiles; complete profiles are at x = 24, 84 in.

(d) flows 6100, 6300 (Bauer 1951, 20°, 60° slope); last 10, 8 profiles; complete profiles are at x = 7 ft, 20° slope and at x = 12 ft, 60° slope.

(e) flows 1100, 1200 (Ludwieg and Tillmann 1949, moderate or strong positive pressure gradient); last 10, 8 profiles (except x = 3.932 m omitted, flow 1200); complete profiles are at x = 1.782 m, moderate gradient and at x = 3.732 m, strong gradient.

(f) Preston-tube calibration in pipe flow (Patel 1965).

Notes for figure 3:

(a) flow 2300 (Clauser 1954, flow 2); 8 profiles; $\Pi \sim 4.13$.

(b) flow 2600 (Bradshaw and Ferriss 1965, a = -0.255); flat pitot tube; 4 profiles; $\Pi \sim 2.99$.

(c) flow 2600a (Bradshaw 1966, a = -0.255); round pitot tube (displacement correction removed); 2 profiles, $\Pi \sim 2.99$. One sour point suppressed in fitting.

(d) flow 2200 (Clauser 1954, flow 1); 8 profiles, renormalized; $\Pi \sim 1.71$.

(e) flow 2500 (Bradshaw 1966, a = -0.150); round pitot tube (displacement correction removed); 4 profiles; $\Pi \sim 1.20$.

Notes for figures 4 and 5:

(a) flow 1400 (Wieghardt 1944, constant pressure); last 15 profiles; $\Pi \sim 0.62$.

(b) flows 5400, 5500,5800, 5900 (Klebanoff & Diehl 1951); last 4, 2, 4, 4 profiles; $\Pi \sim 0.60$.

(c) flows 6100, 6300 (Bauer 1951, 20°, 60° slope); small pitot tube; last 10, 8 profiles; $\Pi \sim 0.30$.

(d) flow 6200 (Bauer 1951, 40° slope); large pitot tube; last 9 profiles; $\Pi \sim 0.26$.

(e) flow 1300 (Ludwieg and Tillmann 1949, $dp/dx < 0$); last 8 profiles; $\Pi \sim 0.24$.

Notes for figure 6:

(a) flows 5200, 5300 (Stratford 1959, experiments 5 and 6); last 3, 3 profiles.

(b) flow 3500a (Newman 1951); 7 profiles (turbulence correction removed).

(c) flow 2900 (Perry 1966); 10 profiles (last profile incomplete).

(d) flows 1100, 1200 (Ludwieg and Tillmann 1949, moderate or strong positive pressure gradient); last 10, 8 profiles ($\Pi \geq 1$)(except $x = 3.932$ m omitted, flow 1200).

(e) flows 6400, 6500, 3300 (Bradshaw 1967, $a = 0 \rightarrow -0.255$, layers A, B, C); displacement correction removed; last 7, 6, 6 profiles ($\Pi \geq 1$). Two sour points suppressed in fitting.

Notes for figures 8 and 9:

(a) flows 1700, 1800 (Gruschwitz 1931, Messreihe 4, 5); profiles for $59.3 \leq x \leq 71.7$ cm, $84.35 \leq x \leq 96.7$ cm ($\Pi \geq 1$).

(b) flow 3200 (Bell 1966, flow E); last 7 profiles ($\Pi \geq 1$).

(c) flow 3000 (Bell 1966, constant pressure); last 9 profiles; $\Pi \sim 0.63$.

(d) flow 1500 (Tillmann 1945, ledge); last 6 profiles; $\Pi \sim 0.09$.

(e) flow 1600 (Riabouchinsky 1914); last 5 profiles (data incomplete at outer edge of layer); $\Pi \sim 0.85$.

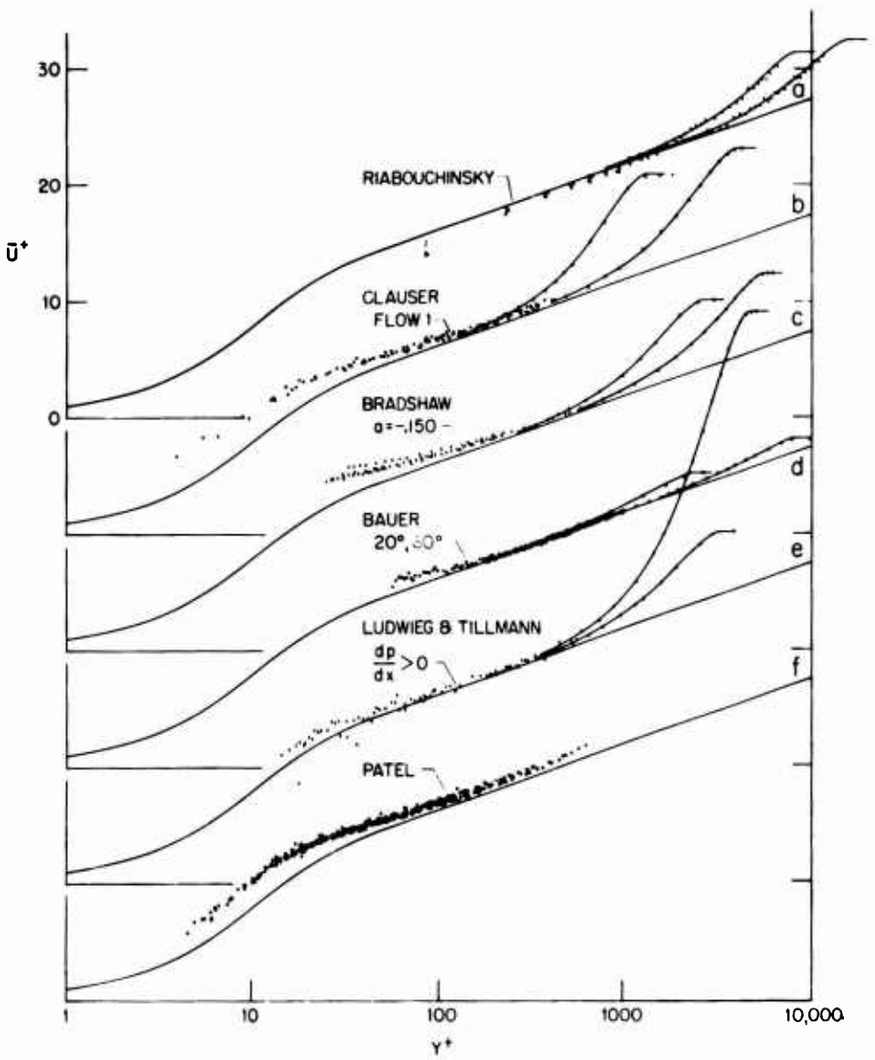

Figure 1. Data from several sources in the coordinates of the law of the wall. The lowest curve (f) is Patel's (1965) Preston-tube calibration in pipe flow. Each of the other curves shows all of the data points near the wall which were not used in the fitting operation, together with two complete profiles for reference.

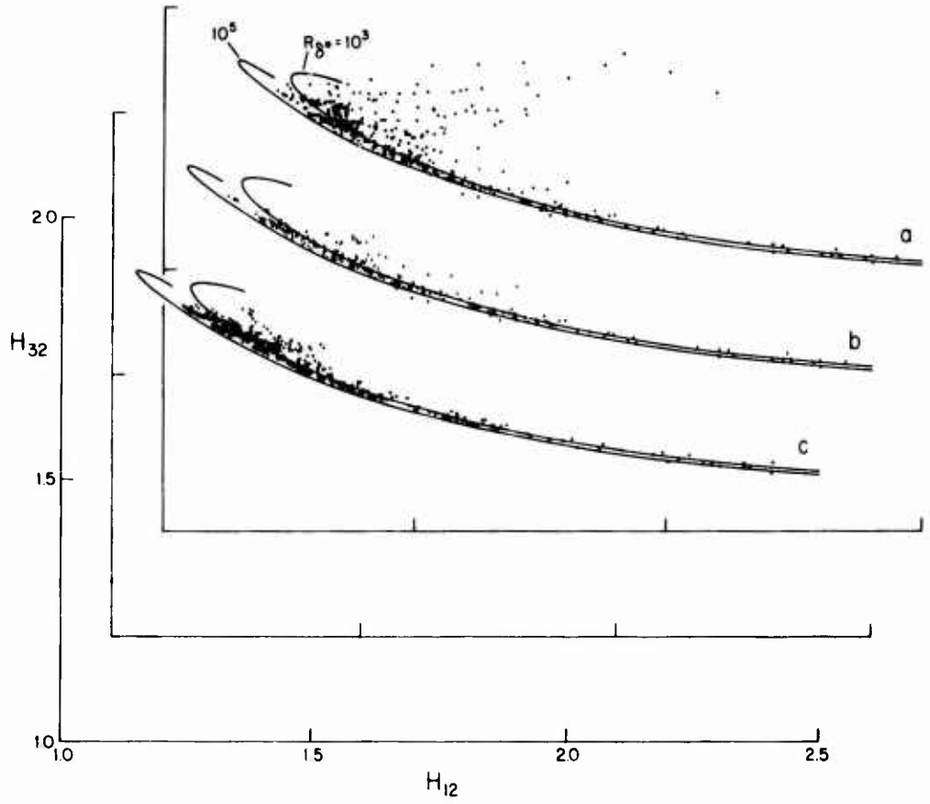

Figure 2. Evaluation of integral thicknesses by different methods. Curve (a) shows values obtained by Coles and Hirst, using parabolic interpolation in the sublayer (cf Volume II of the proceedings of this conference). Curve (b) is the same except for omission of data for which the profile is not experimentally defined near the wall. Curve (c) again shows all of the data, as in curve (a), but with values obtained using a standard sublayer profile (cf Table I of this survey). The solid lines correspond to equations (1)-(3), which assume a logarithmic profile in the sublayer.

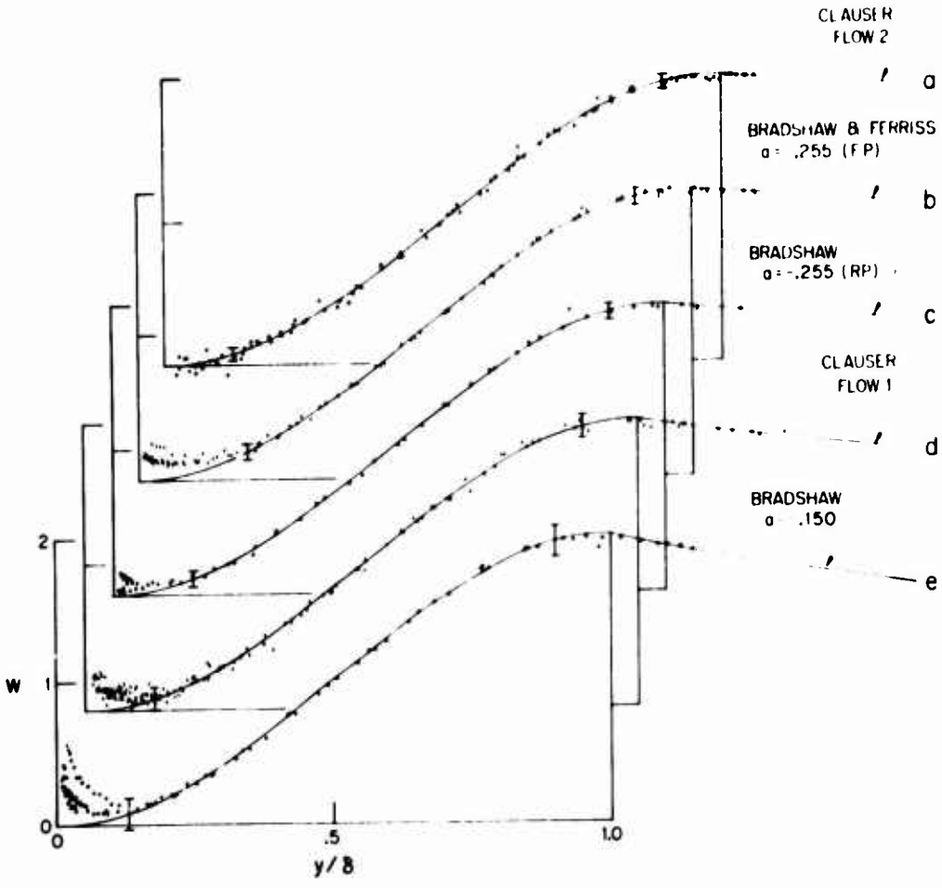

Figure 3. The wake component for equilibrium flow in a positive pressure gradient. The vertical bars show the limits of the fitting region and also show the relative size of a velocity increment of 0.01 $\bar{U}_\infty$. Points with $yu_\tau/\nu < 50$ are omitted.

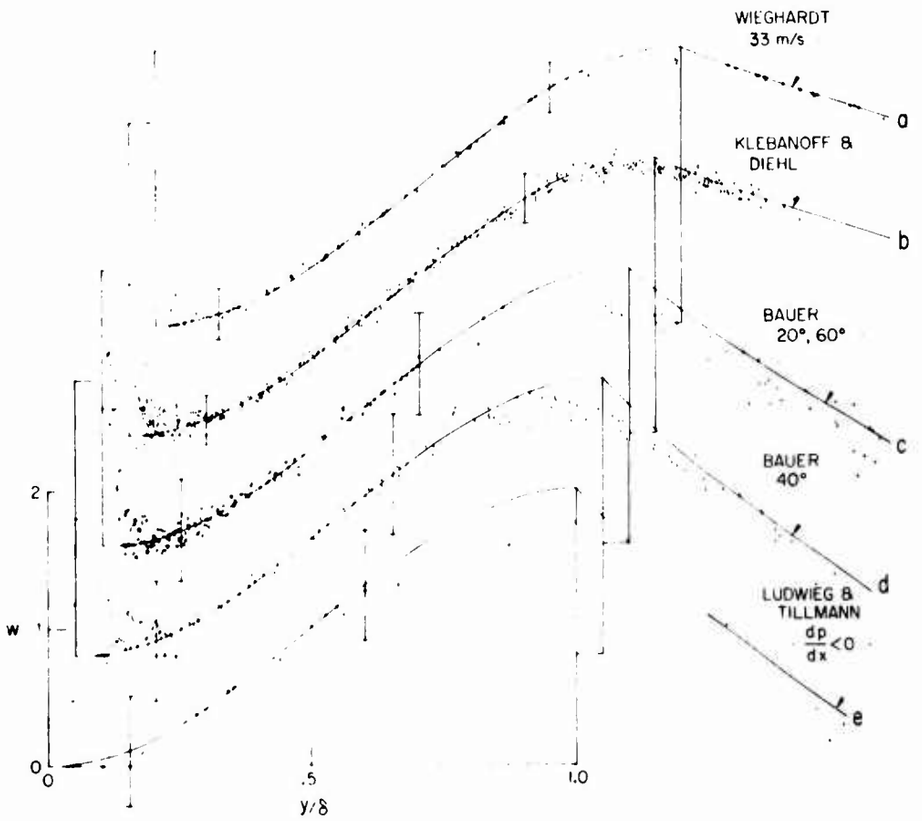

Figure 4. The wake component for equilibrium flow in a zero or negative pressure gradient. The vertical bars show the limits of the fitting region and also show the relative size of a velocity increment of 0.01 $\bar{U}_\infty$. Points with $yu_\tau/\nu < 50$ are omitted.

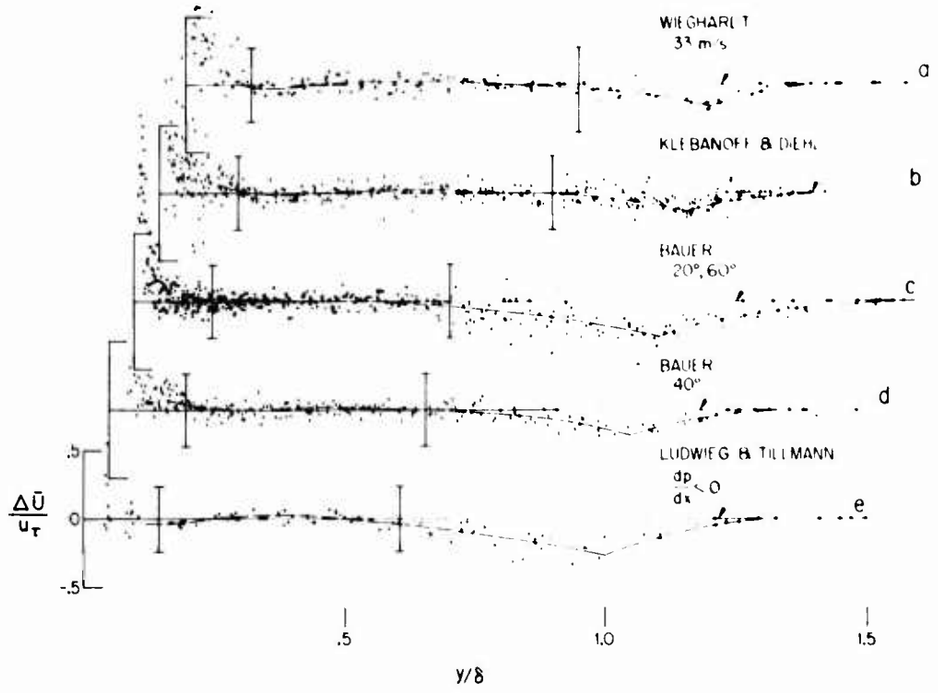

Figure 5. The data of figure 4 replotted as residuals to emphasize discrepancies near the wall and near the free stream. The vertical bars show the limits of the fitting region and also show the relative size of a velocity increment of 0.01 $\bar{U}_\infty$. Points with $yu_\tau/\nu < 50$ are omitted.

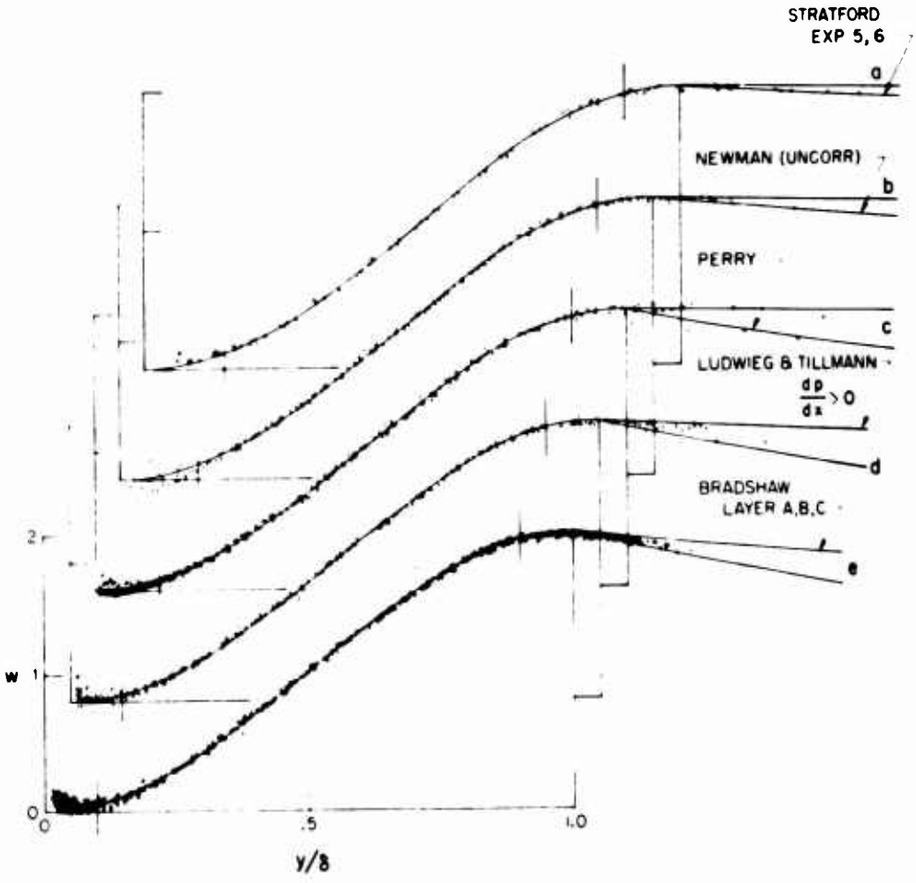

Figure 6. The wake component for several flows of airfoil or diffuser type. The vertical bars show the limits of the fitting region. Points with $yu_\tau/\nu < 50$ are omitted.

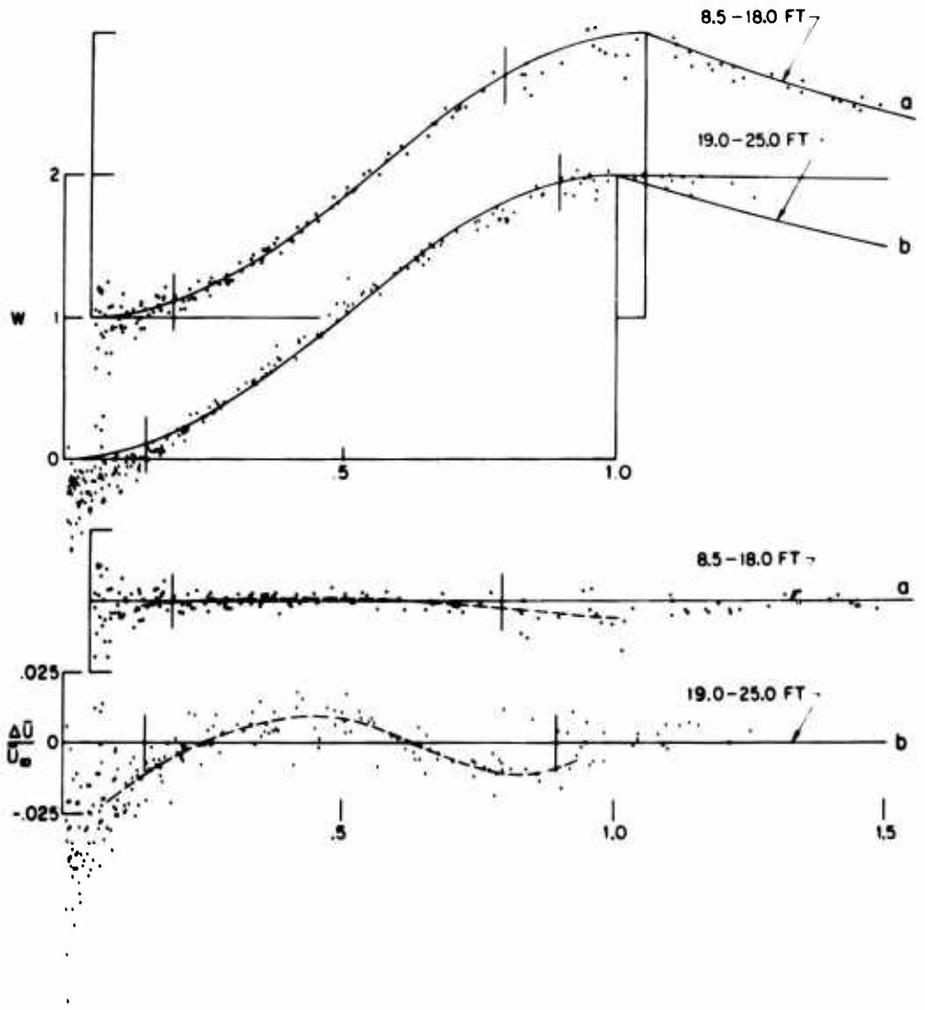

Figure 7. The measurements by Schubauer and Klebanoff (1950) (flow 2100), analyzed separately for (a) the upstream region of flow over a plane surface, and (b) the downstream region of flow over a curved surface of large radius. The vertical bars show the limits of the fitting region. Points with $yu_\tau/\nu < 50$ are omitted.

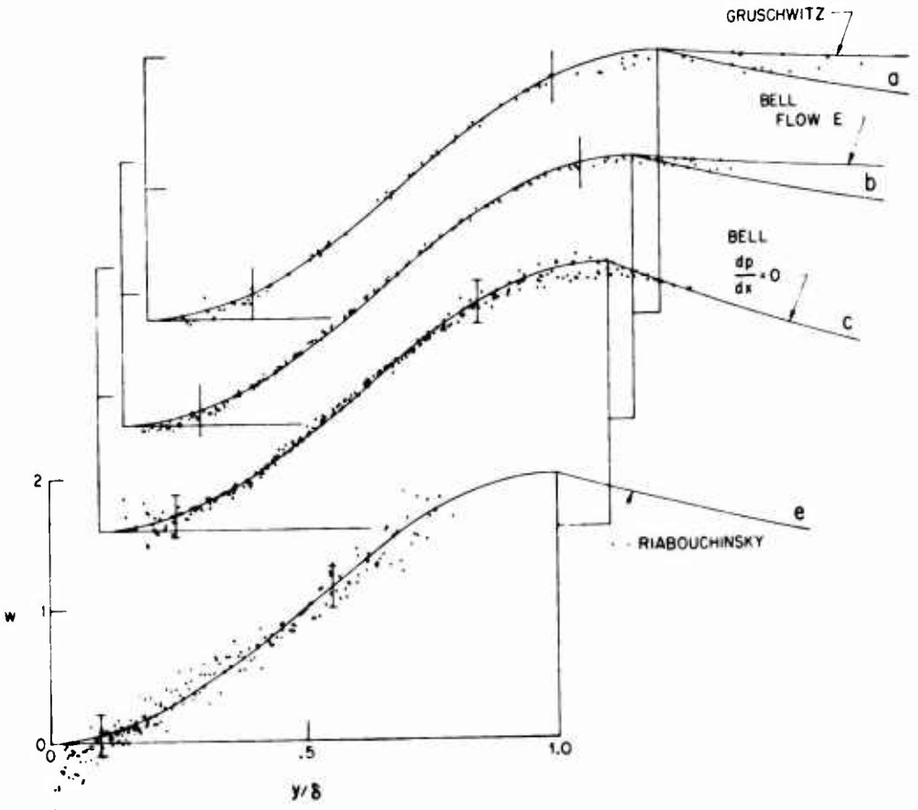

Figure 8. The wake component for several flows showing small anomalies. The vertical bars show the limits of the fitting region, and for the two lower curves also show the relative size of a velocity increment of 0.01 $\bar{U}_\infty$ (0.01 $\bar{U}_w$ in the case of Riabouchinsky's experiment). Points with $yu_\tau/\nu < 50$ are omitted.

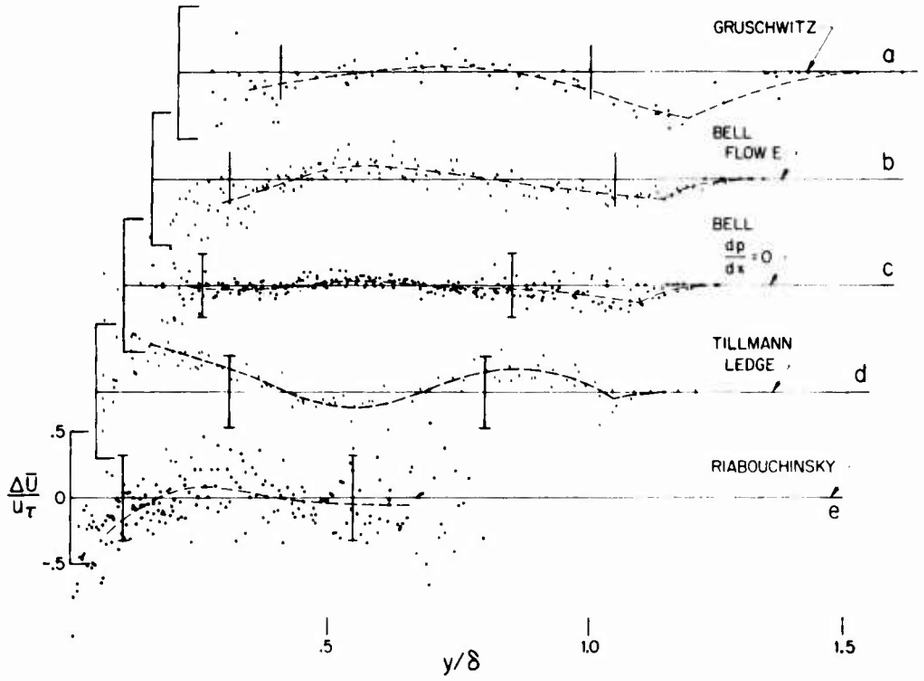

Figure 9. The data of figure 8 replotted as residuals to emphasize the various anomalies. The vertical bars show the limits of the fitting region, and for the three lower curves also show the relative size of a velocity increment of 0.01 $\bar{U}_\infty$ (0.01 $\bar{U}_w$ in the case of Riabouchinsky's experiment). Points with $yu_\tau/\nu < 50$ are omitted.

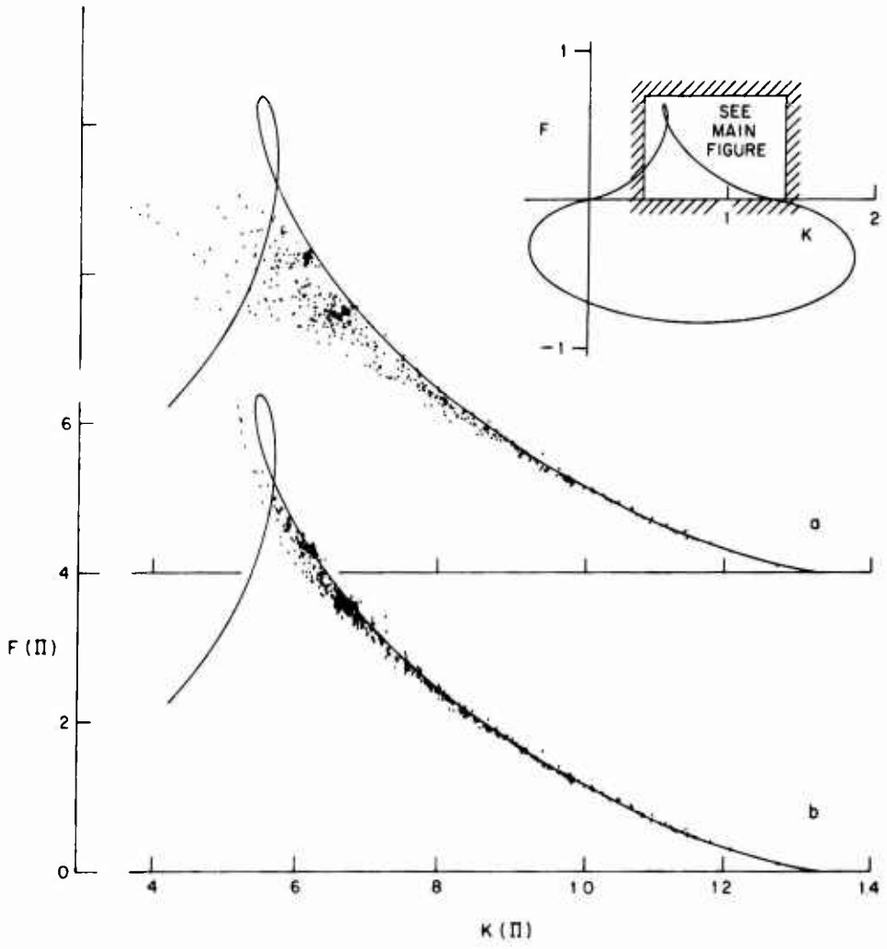

Figure 10. The local friction law F(K). The insert shows the complete analytical curve defined by equations (11) and (12), assuming a logarithmic profile in the sublayer. The data in (a) are placed according to equations (9) and (10), using values of H, f, and R_{δ^*} from Table I. The data in (b) are adjusted by reducing δ^* by 65 $\nu/\bar{U}_\infty$ in both H and R_{δ^*}.

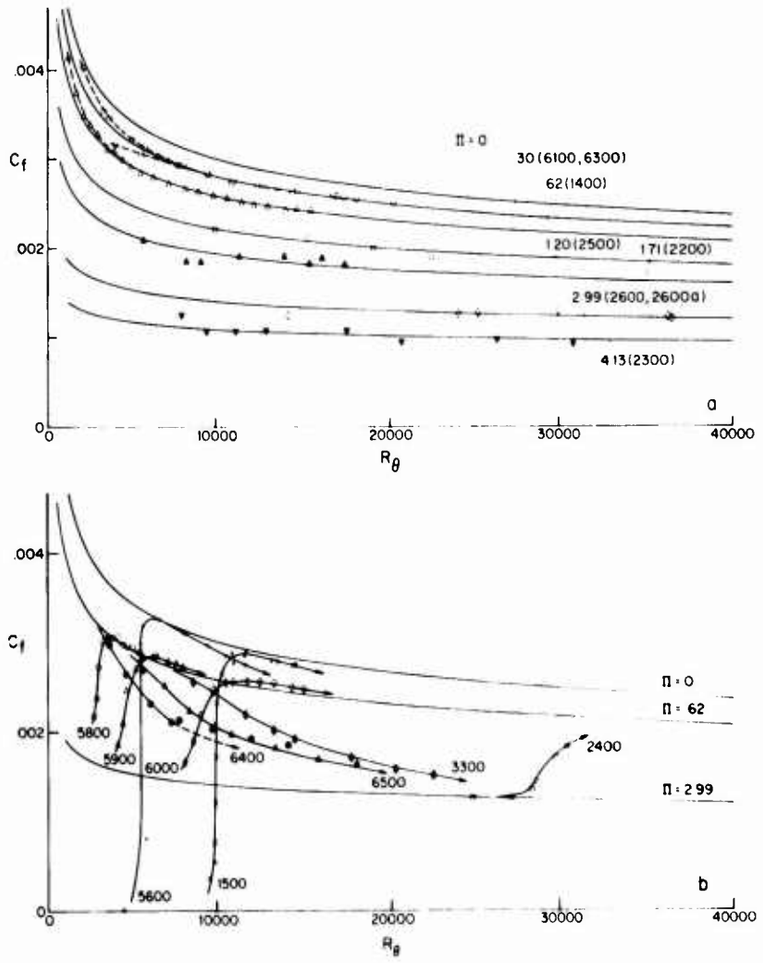

Figure 11. The development of several flows in the coordinates C_f, R_θ. The solid lines representing equilibrium flow are computed from equations (9) and (10) with δ^* reduced by $65\nu/\bar{U}_\infty$ in both H and R_{δ^*}.

6100/6300	Bauer (1951), $20^o/60^o$ slope
1400	Wieghardt (1944), constant pressure
2500	Bradshaw (1966), a = - 0.150
2200	Clauser (1954), flow 1
2600, 2600a	Bradshaw and Ferriss (1965), a = - 0.255
2300	Clauser (1954), flow 2
5800/5900/6000	Klebanoff and Diehl (1951), sand, 35/55/108 ft/sec
5600	Klebanoff and Diehl (1951), 1/4-inch rod
1500	Tillmann (1945), ledge
6400/6500/3300	Bradshaw (1967), layers A/B/C
2400	Bradshaw and Ferriss (1965), a = - 0.255 → 0

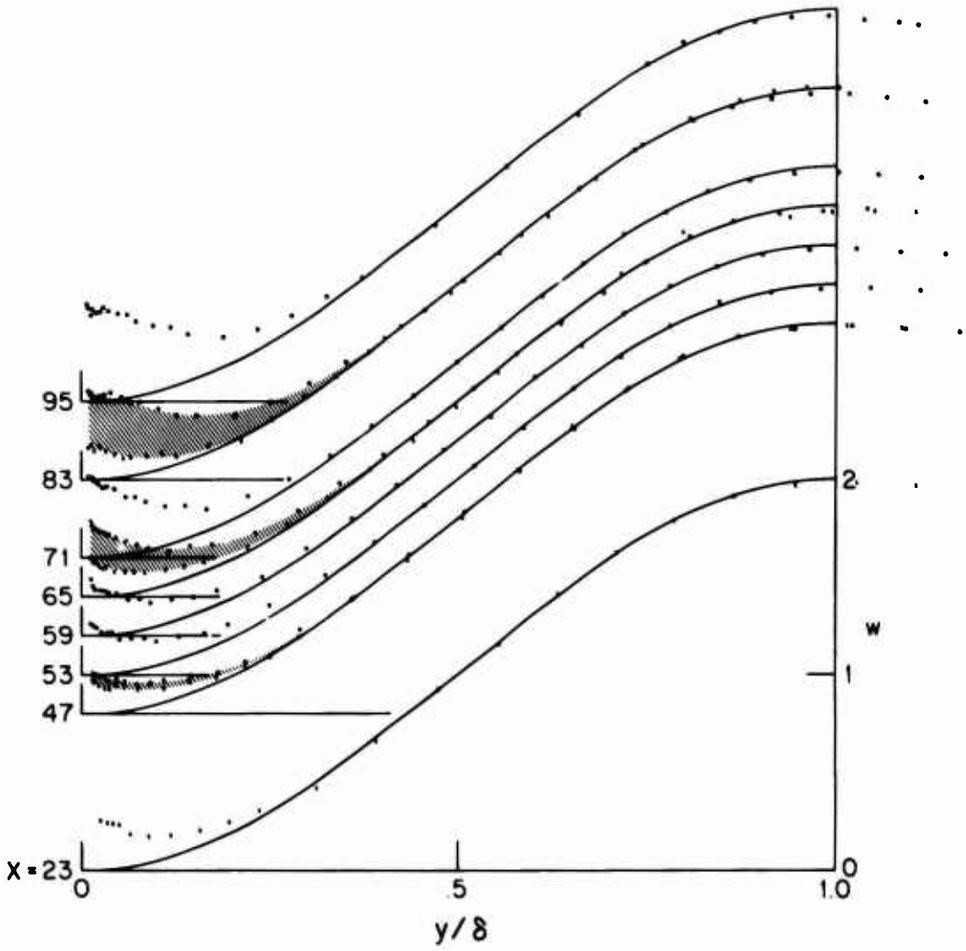

Figure 12. Comparison of the wake component for the equilibrium flow a = - 0.255 (flow 2600) and the corresponding relaxing flow a = - 0.255 → 0 (flow 2400) of Bradshaw and Ferriss (1965).

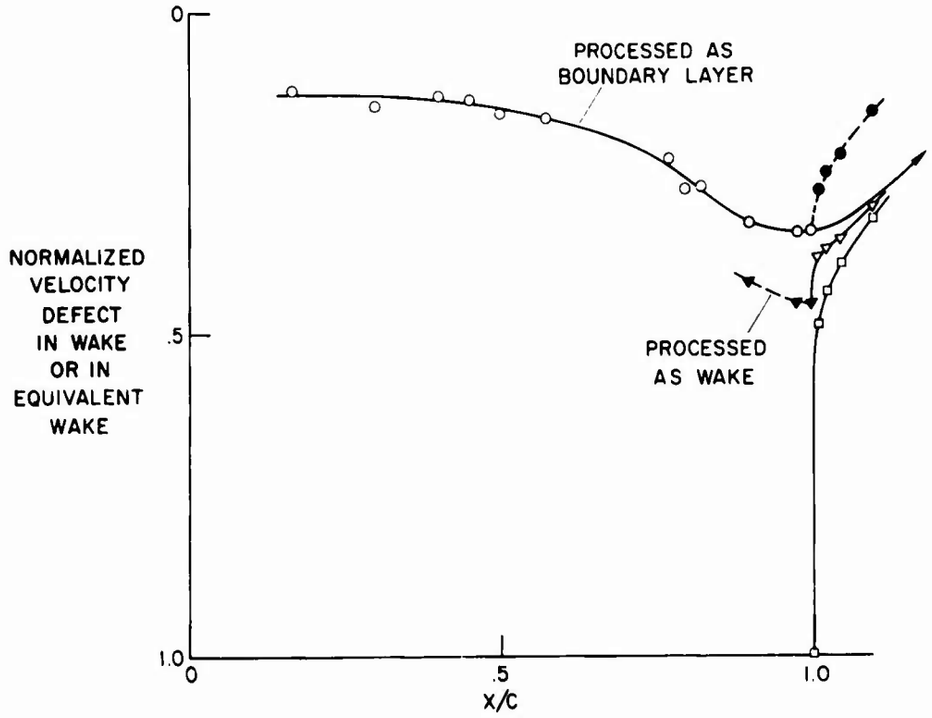

Figure 13. Relaxation process near the trailing edge of an airfoil (Mendelsohn 1947)(flow 4200). The circles show the velocity defect at the wall for the equivalent wake, as established by a boundary-layer fit. The triangles show the velocity defect at the plane of symmetry, as established by a wake fit. The squares show the actual velocity at the plane of symmetry in the wake.